DETERMINING THE TRIBUTARY SEDIMENT CONTRIBUTION TO EXPERIMENTAL FLOOD DEPOSITS ON THE COLORADO RIVER IN MARBLE CANYON, GRAND CANYON, ARIZONA

By Katherine A. Chapman

A Thesis

Submitted in Partial Fulfillment

of the Requirements for the Degree of

Master of Science

In Geology

Northern Arizona University

May 2017

Approved:

Roderic A. Parnell, Ph.D., Chair

Paul E. Grams, Ph.D.

Michael E. Smith, Ph.D.

Erich R. Mueller, Ph.D.

ABSTRACT

DETERMINING THE TRIBUTARY SEDIMENT CONTRIBUTION TO EXPERIMENTAL FLOOD DEPOSITS ON THE COLORADO RIVER IN MARBLE CANYON, GRAND CANYON, ARIZONA

KATHERINE A. CHAPMAN

A multivariate sediment fingerprint was used in a Bayesian mixing model to determine the source contribution to experimental flood deposits along the Colorado River in the Marble Canyon reach of Grand Canyon, AZ. This study provides an independent evaluation, complementary to previous sediment mass balance and morphological studies, of the degree to which sand from the Paria River, the primary source of sand in Marble Canyon, has supplemented total sand storage since upstream dam closure in 1963. Samples of endmember and downstream mixed populations of sand were analyzed using portable XRF to measure the concentration of eleven major and trace elements, from which 55 elemental ratios were calculated. A principal components analysis consolidated those ratios eligible for use in the fingerprint into a multivariate signature used in the mixing model, MixSIAR.

Twenty flood deposits from 14 sites in Marble Canyon from the 2013 and 2014 controlled floods were sampled. Six individual mixing models, using sediment fingerprints unique to each of six half-phi grain size fractions returned the percentage of sand, in each size fraction of each deposit, that was sourced from the Paria River. Paria contribution averaged 33.8 ± 4.1% in deposits from the 2013 flood, and 54.7 ± 4.3% in deposits from the 2014 flood. Individual grain size samples ranged 4.9 – 73.1% in 2013 and 9.1 – 90.2% in 2014. In general,

the four median grain size fractions (90 – 355 μm) in both years have the highest Paria contribution; low Paria contribution in the finest 63 – 90 μm) fraction suggests significant contribution by an unaccounted-for third endmember, likely minor tributaries. The coarsest fraction, 355 – 500 μm, is the only grain size to show a trend in Paria contribution with distance traveled downstream, suggesting a transport-related fractionation effect. Overall scatter in the results speaks to the spatial heterogeneity of intra-rapid storage pools throughout the reach and their capacity, as well as the effects of local hydraulic variability between eddy deposition zones where sandbars form. Mass balance calculations determine that under conditions of constant or decreasing total storage since 1963, approximately 20-30% of the annual Paria flux would need to be retained within Marble Canyon each year to reach the observed concentration of Paria sand. From these results, we conclude that HFEs are conditionally sustainable given frequent enough occurrence to maintain sandbar deposit storage.

ACKNOWLEDGEMENTS

This thesis would not have been possible without the help and support, in the field and office alike, from many individuals. I could not have asked for a better advisor than Rod Parnell. A month into my time at NAU on my first research trip in the Grand Canyon, I realized how fortunate I was to have been given an opportunity to work with him and in the three years following was never led to believe otherwise. My committee, Paul Grams, Mike Smith, and Erich Mueller deserve a heartfelt thank you for the wide range of perspectives, experience, and guidance they brought to this project. I'd like to extend an extra thank you to Mike Smith for bringing me into his syndicate group and providing guidance when Rod could not be there, and for the delicious organic lunch meat on field trips.

Many individuals outside my committee were essential to the success of this project as well. I would have certainly drowned in the copious amounts of data I collected had it not been for Nick McKay and his enthusiasm for data analysis. I hope to continue to use the coding skills I learned from him for the rest of my career, and this project would not have been possible without that knowledge and the statistical expertise he consistently offered. Becca Best was instrumental to the success of this project as well, helping me understand the world of Bayesian statistics and interpreting the inner workings of MixSIAR. She came through in critical times just days before conferences or presentations on multiple occasions and this project would not have been near as impressive, thorough, or robust without her help.

Research trips rafting in the Grand Canyon are almost guaranteed to be enjoyable, though the crew of people at the Grand Canyon Monitoring and Research Center and NAU that partake in the annual sandbar trips are bar-none the best field buddies out there. Matt Kaplinksi and Joe

Hazel, thank you for not only welcoming me into the NAU's sandbar studies project but trusting me with a boat, teaching deep respect for the golden rule, and above all else, getting the data. Rynam, K-nam, and Gaipan: you taught me how to nam, I found a piece of myself crunching celery and wading through offshore glory with you guys. Namaste. To the gunners, Rob, Keko, Joey, and Rod, Melada, and Coop: you'll never know how much I love springing into action, running to my next point at the ever-so-fast click of the radio or "gooooooooood" floating across the river. And to Fritz and Grand Canyon Youth, for the opportunity to teach kids to love sand and read its secrets.

And finally, to Jon, who not only put up with an extra, unintended third year of grad school, but was beyond supportive the entire time. Understanding when I couldn't leave the lab even after 12 hours of zapping sand with x-rays and instead bringing a pizza dinner date to me, understanding that I sometimes stress about unnecessary things and bringing me back to Earth, and his enthusiasm and pride sharing my work. To my family, understanding that the river is my home, I hope to take all of you down the river again. You are, after all, the ones I first got to go down there with.

Funding for this project came from many sources. The NAU Friday Lunch Clubbe provided funding through a most unique application writing opportunity as well as the Bedwell award and Montgomery Prize, and Geological Society of America. The Hydro Research Foundation was instrumental in allowing me to finish this project with three fully funded years, as well as insight into the world of hydropower I never would have had otherwise. Further support from NAU sandbar studies and GCMRC made this project and all the research trips possible, as well as inspiring me towards further work as a scientist who goes boating.

CONTENTS

LIST OF TABLES

LIST OF FIGURES

PREFACE

This thesis is presented in three chapters: 1) an extended introduction explaining the broad scope of Grand Canyon studies within which the project fits, 2) a detailed methods section from which the exact techniques used in this study can be replicated, and 3) a standalone manuscript intended for publication. There is repetition between the three chapters. Each document has its own Works Cited, formatted under the guidelines of the Geological Society of America. There is no fourth chapter containing an overall discussion of results and conclusions, this is contained within the manuscript chapter. Comprehensive mixing model diagnostics are available as a supplementary file.

CHAPTER 1: INTRODUCTION

Geomorphic Impacts of Dams

While often providing crucial support for human infrastructure through hydropower production, water storage, and flood control, dams are also widely recognized for their disruption of fluvial systems across the world. Impacts of these structures can be both spatially and temporally extensive, with sustained geomorphic responses often seen far downstream (Petts, 1980; Williams and Wolman, 1984). The root cause of these near-permanent adjustments of the downstream fluvial geomorphology is intrinsic to the design of large dams especially and their ability to disrupt the supply of sediment from above to below the dam and exert a high degree of control over the natural flow regime (Lane, 1955; Petts, 1980; Petts and Gurnell, 2005). A wide range of geomorphic adjustments can occur as a result of this control, determined primarily by the relative degrees to which the sediment supply for and transport capacity of the river change, also described as the sediment mass balance (Williams and Wolman, 1984; Graf, 2006, Schmidt and Wilcock, 2008).

Patterns are evident in the direct effects of dams on the hydrologic and sediment regimes of rivers, however the consequently affected channel geomorphology of impacted reaches tend to have more varied responses and can be difficult to predict (Petts, 1980). In a comprehensive study of 36 very large dams throughout many different climates and regions in the US, Graf (2006) found that, among other statistics, peak annual flows on impounded rivers are significantly decreased (reduced by 67%), the magnitude of minimum flows increase by 52%, and the number of flow reversals increase by 34%. Additionally, the timing of these minimum and maximum flows shifted by up to six months from their typical pre-dam seasonal occurrence. Significant dam-induced changes such as these are not unique to large dams and rivers: in a

study of 21 dams of varying size and contributing watershed area, Magilligan and Nislow (2005) found that dams consistently affected all Indicators of Hydrologic Alteration as described by Richter and others (1996). Dams such as these also trap effectively all sediment delivered from upstream of the dam, typically leaving the downstream reach sediment starved (Williams and Wolman, 1984; Syvitski et al., 2005). Geomorphic responses to these changes vary greatly, with channels often either widening or narrowing as a function of many drivers, including altered sediment transport processes and channel size and functionality, often reinforced by the response of vegetation and its consequent influence on sediment transport (Graf, 2006).

Impacts on Colorado River below Glen Canyon Dam

In close alignment with these general trends, the 1963 completion of Glen Canyon Dam on the Colorado River (Fig. 1) significantly altered the hydrologic and sediment regimes of the downstream river, causing demonstrable channel adjustment throughout the length of Glen and Grand Canyons. Dolan and others (1974) first documented the extent of these changes, describing them as both "rapid and significant", posing questions about the nature of these changes and how quickly the river was adjusting. Since then, many studies have investigated the details of these changes and channel responses; summarized below are the results which pertain to the Marble Canyon reach of Grand Canyon (Fig. 1), the reach closest to the dam and the focus of this study.

Changes to the Hydrologic Regime

The natural hydrologic regime of the Colorado River in Grand Canyon was highly variable, with flows fluctuating by several orders of magnitude over the course of a typical year. In general, spring snowmelt floods originating in the high elevations of the upper basin drove the

river to its maximum discharge each year around May and June (Dolan et al., 1974). Snowmelt floods with a two-year recurrence interval 85,000 cfs (2350 m^3/s), floods of approximately 120,000 cfs (3,400 m^3/s) occurred about every 6 years, and the two largest observed floods were 210,000 cfs (5947 m^3/s) in June 1884 and 170,000 cfs (4814 m^3/s) in June 1921 (Topping et al., 2003; Schmidt and Grams, 2011a). Flash floods in the late summer and fall were of a much shorter duration and smaller magnitude than spring snowmelt floods, though these floods carried a much higher sediment flux than spring snowmelt floods (Dolan, 1974; Topping et al., 2000a). Between these seasonal floods, however, the river was consistently characterized by flows less than 3,000 cfs (Topping et al., 2000a).

These patterns of seasonal variation, the range of flows, and the time period over which those flows fluctuated, were significantly altered by Glen Canyon Dam. On the newly regulated river, daily releases were dictated by power needs and varied dramatically throughout the day. From 1963 to 1991, releases ranged from less than 5,000 cfs to about 31,000 cfs (140-880 m^3/s), which is near the maximum power plant capacity (Webb et al., 2005). These releases were different from the natural flow in two main ways, concerning daily fluctuations and average flow magnitude. Compared to the low pre-dam daily flows, the post-dam daily flows were of a much greater magnitude, with a 58% increase in median flow (Topping et al., 2003; Schmidt and Grams, 2011a). Additionally, spring flood magnitude decreased to about 63% of the average pre-dam peak discharges. Large daily variations in power demands led to a median daily range in discharges around 8,580 cfs (243 m^3/s) which was not only much greater than the pre-dam range of approximately 524 cfs (15 m^3/s), but also greater than the annual pre-dam median discharge (Topping et al., 2003, Webb et al., 2005). The post-dam daily range in discharge was greater than

10,000 cfs (283 m^3/s) on 43% of the days, whereas the pre-dam river had a range this large only 1% of the time (Topping et al., 2003).

There were some interruptions to the post-dam power-generating releases: in 1965 a series of short burst "pulse" flows, six of which were over 50,000 cfs (1416 m^3/s), were released with the intent of equalizing the volume of water stored in Lakes Powell and Mead (Grams et al., 2007). Then, in 1983 to 1986, a series of exceptionally large snowmelt floods in the upper basin led to large releases over power plant capacity used to manage reservoir volume in Lake Powell. The largest of these, in 1983, had a maximum release discharge of 91,300 cfs (2585 m^3/s) and a total duration over one month (U.S. Department of the Interior, 1996; Schmidt and Grams, 2011). The first environmentally-driven flow experiments occurred over a 13-month period in 1990-91, where bar topography was measured following 2-week long blocks of varied hydrograph shapes (Schmidt and Grams, 2011). The goal of these flows was to investigate the potential utility of manipulating dam releases for the sake of downstream restoration and were followed in 1996 by a protocol known as Modified Low Fluctuating Flows (MLFFs). MLFFs restricted the range of flows released over a 24-hour period to 5,000-8,000 cfs (142-227 m^3/s), depending on the current power release schedule (Schmit et al., 2005, Wright et al., 2005). These guidelines currently dictate daily flows which are now punctuated by management-driven "floods" discussed in detail in a later section.

Sediment Supply and Transport: Pre- vs. Post-Dam

Prior to the completion of Glen Canyon Dam, sediment originating from within the entire upper Colorado River basin was delivered through Glen Canyon, past Lee's Ferry, and downstream into the Marble Canyon Reach of Grand Canyon (Fig. 1). Based on the years 1949-1962, estimates of the annual upper basin sediment flux are around 57 million Mega grams (Mg,

equivalent to 1 metric ton) per year. The Paria River, with its confluence just downstream of Lee's Ferry, supplies an additional average of 1.5 million Mg of sediment annually to Marble Canyon (Topping et al., 2000a). Further downstream, the Little Colorado River supplies, on average, 1.9 million Mg of sediment per year. Its confluence with the main stem Colorado River marks the downstream end of the Marble Canyon reach of Grand Canyon, thus Marble Canyon does not benefit from this sediment flux (Wright et al., 2005, Topping et al., 2000a).

Patterns of pre-dam aggradation and scour were largely controlled by seasonal variability in discharge when relatively low flows of late summer, fall, and winter limited the transport capacity of the river (Dolan et al., 1974, Topping et al., 2000a). Monsoon floods in the summer introduced large influxes of sediment, which accumulated in the channel until the higher spring flows. Spring snowmelt floods mobilized this sediment and transported it downstream (Topping et al., 2000a; Webb et al., 2000; Wright et al., 2005). The misalignment of these periods of high transport capacity and high sediment flux meant that the pre-dam river was fine sediment supply limited within time frames less than one year. Evidence for this pre-dam sediment supply limitation is further supported by the extensive analysis by Topping and others (2000a, b) of historical hydrographs, suspended sediment concentrations, bed elevation data, and pre-dam flood deposits. The pre-dam river showed a coupled hysteresis with discharge in spring snowmelt floods by both grain size and sediment concentration, indicating that these floods were fine sediment supply limited. Additionally, pre-dam flood deposits were often inversely graded and there were consistent lags between the minimum and maximum bed elevations compared to the flood peaks, both of which suggest fine sediment supply limitation (Rubin et al., 1998; Topping et al., 2000a).

Though the pre-dam river showed signs of fine sediment supply limitation, the same effects were far more prevalent and extreme in the post-dam river. Glen Canyon Dam effectively blocks all sediment delivery from the upper basin, cutting off over 93% of the pre-dam sediment supply to Marble Canyon. Now, the relatively small volume of sediment supplied by the Paria River comprises over 90% of the total available sediment to Marble Canyon, making it more severely fine sediment supply limited (Topping et al., 2000a). This reduction in sediment supply is quantified by measured sediment flux data through Lee's Ferry: in 1963, 20 million Mg of sediment passed the Lee's Ferry gage (upstream of the Paria confluence), followed by 4.0 and 5.0 million in 1964 and 1965, respectively. The average annual sediment load passing through Lee's ferry in the years 1966-1970 was 0.24 +/= 0.01 million Mg, which is a >99% reduction from pre-dam levels. This sediment flux through Lee's Ferry in the few years after the dam was completed is associated with observed bed-armoring in the remaining stretch of Glen Canyon below the dam (Dolan et al., 1974, Topping et al., 2000a; Grams et al., 2007). The current sediment flux past the Lee's Ferry gage is negligible (Grams et al., 2007).

Resulting Morphologies: Pre- vs Post-Dam:

In Marble Canyon, flows less than 9,000 cfs are required to accumulate sand, as flows greater than that result in large scale sediment transport (Topping et al., 2000a). The pre-dam river exceeded this threshold only 44.3% of the time, whereas the post-dam river exceeded this threshold 52.7% of the time in the late 1960s, increasing to 88.2% of the time in the 1990s (Topping et al., 2000b). This change in conditions is largely to blame for the large differences seen in the pre- versus post-dam channel morphologies in Marble Canyon.

Prior to the dam, the channel was lined with a series of terraces and bars corresponding to the pre-dam annual and two-year floods (Dolan et al., 1974). These deposits were located at the

mouth of tributary canyons mainly as debris fan eddy sandbars, but also as point bars and marginal deposits along straight stretches of the river (Dolan et al, 1974). Snowmelt floods would typically cause channel scouring of the sand that had aggraded during monsoon season, with the minimum bed stage at Lee's Ferry fluctuating approximately 2 m annually (Topping et al., 2000a). Overall, aggradation generally balanced scouring, resulting in a dynamic morphology that responded to the seasonal variations in discharge, the corresponding transport capacity, and sediment supply.

Following the completion of Glen Canyon Dam, the altered hydrologic regime and sediment supply led to the degradation of downstream channel deposits. Both the areal extent and overall elevation of these deposits decreased, some sandbars all but disappeared, and vegetation began taking hold in areas no longer inundated during annual floods (Dolan et al., 1974). Engineers had successfully predicted the channel erosion that took place immediately below the dam, though the downstream extent to which this erosion would ultimately reach was unclear at the time. Results of post-dam investigations varied widely, predicting overall channel aggradation (Howard and Dolan, 1981), an approximate equilibrium of sand export and supply (Andrews, 1990), and overall channel erosion (Laursen et al., 1976). The variation in these predictions was due largely to differences in estimated tributary sediment supply from the Paria River (Laursen et al., 1976; Randle and Pemberton, 1987) and the river's transport capacity, thus underlining the need for a greater understanding of the sediment supply, storage, and transport processes taking place in the post-dam Colorado River.

Evolution of Current Research and Management

Beginning in 1990 scientific research began to take its place within the management and restoration framework in which it exists today. In 1990 and 1991, the first experimental flows

with the goals of learning more about physical processes and restoration potential in Grand Canyon took place as part of the Glen Canyon Environmental Studies in efforts to create the Environmental Impact Statement (EIS) for Glen Canyon Dam. A series of thirteen 2-week long test flows with varying hydrograph shapes were released, followed by interim low flows where the responding channel geomorphology was documented. In these studies, Beus and others (1992) observed that the antecedent sand supply and its interaction with transport capacity to affect suspended sediment concentration had a much stronger control on bar behavior than discharge alone. Recognizing the benefits of a formal organization through which scientific research could continue and be used to inform dam operations, the Grand Canyon Monitoring and Research Center (GCMRC) was established as part of the Glen Canyon Dam Adaptive Management Program (GCDAMP) in the 1996 Record of Decision for the Operation of Glen Canyon Dam. The GCDAMP outlines how scientific findings by GCMRC should be used to determine ways in which Glen Canyon Dam should be operated in to achieve specific goals for downstream resource restoration.

The Record of Decision implemented two major changes to the previous release patterns from Glen Canyon Dam: introduction of Modified Low Fluctuating Flow (MLFF) regulations, and periodic Beach Habitat Building Flows, or BHBFs. MLFFs described restrictions on the daily minimum and maximum, flux, and maximum up-/down-ramp rates for flows released from the dam (U.S. Department of the Interior, 1996). The first BHBF did not technically meet the definition of a post-dam “flood”, where power plant capacity must be exceeded for a period of one month or greater, but was the largest controlled release since the floods of the early-mid 1980s (Fig. 2). Lasting for seven days with a constant release of 45,000 cfs, the flood was meant to 1) investigate the viability of dam release floods as a viable option for restoring downstream

resources, and 2) give scientists an opportunity to learn about the physical processes taking place within the post-dam river and use that knowledge to amend future releases. These goals were considered "achieved", at least partially, in that the channel morphology had significantly changed and a great deal of knowledge about flood- and sediment-related processes had been acquired. Topographic surveys by Hazel and others (1999) reported that high elevation areas of the bars had increased in volume and area by 164% and 67%, respectively. In contrast, the lower elevation volume and area of the bars increased by only 37% and 5%, respectively. Schmidt and others (1999) attributed this to the tendency of bars to scour out sand from lower elevations and redeposit it in higher elevations during the flood, only to have it quickly eroded through mass wasting events shortly after the flood. The increased sandbar volumes and areas were short-lived as well, as mass-wasting events eroded bars back to near their pre-flood sizes relatively quickly following the flood (Schmidt, 1999). Despite the temporary lifespan of the rebuilt sandbars, the studies still yielded information about sediment transport processes integral to sandbar management and led to revision of some fundamental theories on which the dam-release flood was designed.

Fluvial systems are inherently complex, and as suggested by Magilligan and Nislow (2005), the success of management efforts is dependent on customizing flood releases to mimic the unique pre-dam conditions necessary for restoring pre-dam channel morphology. In light of this complexity, the adaptive nature of GCDAMP was created specifically to allow scientific findings to continually optimize management actions. Studies following the 1996 BHBF helped determine what optimal management would look like in Grand Canyon and were used as guides for the first adjustments to the flood protocol. Schmidt (1999) focused on one component of the theory behind the 1996 Record of Decision that was inaccurate, citing incorrect assumptions

about sediment transport and supply that had led to the false conclusion that tributary-supplied sediment would aggrade in the channel over the course of multiple years. In truth, sand ultimately scoured from upstream reaches was deposited in downstream reaches and, supporting his reasoning with the conclusion by Wiele and others (1999) that bar topography is related to suspended sediment concentration, Schmidt (1999) proposed a shorter flood duration as a better fit for the time-dependent, reduced sediment supply. Rubin and others (2002) built on this proposal, elaborating on the inaccuracies of the assumption that sediment accumulates over the course of multiple years and emphasizing that changes to the original flood protocol must be made in order to achieve the management objectives of the GCDAMP.

The 2004 and 2008 floods

The next two major flood events, called High Flow Experiments (HFEs), occurred in 2004 and 2008 and were designed to utilize lessons learned during the 1996 BHBF. Fully embracing the concept of antecedent sand enrichment (ASE), scientists aimed to maximize eddy-sandbar storage and minimize the volume of sand pushed through towards Lake Mead by ensuring that the flood duration did not outlast the ASE (Schmidt and Grams, 2011b). The channel in Grand Canyon contains an unknown amount of preserved pre-dam sand, though Topping and others (2000a) consider it unlikely that the total storage increased between 1963 and the 1996 BHBF. In consideration of this, the ASE supplied by the Paria River to Marble Canyon was the primary factor determining the hydrographs for the 2004 and 2008 HFEs. The minimum sediment supply during HFEs is the Paria-derived ASE, as the Little Colorado River cannot supplement main channel sediment until the end of Marble Canyon about 100 km downstream. In effect, this approach acknowledges the sediment supply limitation that was

observed and affected sediment transport patterns during the 1996 BHBF, but was also present in the pre-dam river (Rubin et al., 1998; Topping et al., 2000a).

The bar-building results from these two floods improved upon those from the 1996 BHBF, and additional insight into sediment related processes was gained as well. According to Hazel and others (2010), bar responses fell into one of four categories of spatial patterns in deposition and erosion, and each successive flood had increasingly large percentages of favorable bar responses. Favorable bar responses are defined here as those characterized by deposition above the 8,000 cfs reference stage, which are two of the four possible responses. The underlying lessons learned from the 2004 and 2008 HFEs include: 1) it is possible to consistently aggrade eddy-sandbar deposits though they consistently erode within one year or less of interim flows, and 2) sandbar deposition levels correlate to suspended sediment concentration during the flood, which is a function of ASE volume, the channel area covered, and the grain size distribution of that sand (Topping et al., 2010). In the long term, whether bar size will increase or decrease depends on the magnitude of deposition during HFEs, the frequency of high flows, and the rate of erosion between high flows (Schmidt and Grams, 2011b).

These findings helped guide a new HFE protocol, to be tested out during the ten-year period of 2011 through 2020 (Department of the Interior, 2011). Thus far, HFEs have occurred in November of 2012, 2013, 2014, and 2016, each one shortly after Paria sediment is introduced during the late summer monsoon season of each year (Figure 3). Timing the floods like this maximizes the total ASE available for use by avoiding non-flood downstream transport as much as possible. Results from topographic surveys after each of the floods confirm the prediction that repeated flood events will continue to maintain sandbar size and volume, though the individual sandbar response remains varied. Grams and others (2013) attribute this variance largely to local

hydraulic effects, and stress the shortcomings of extrapolating data from individual sites to entire reaches for morphological sediment budgets. Nevertheless, a sediment budget based on morphological data from a compilation of short reaches showed the same trends as a reach-long flux based sediment budget that used continuously collected suspended sediment data. Neither budget showed a decreasing trend in Marble Canyon sediment storage, though the authors do note that the magnitude of the trend could not be determined without large uncertainties (Grams et al., 2013). These results do, however, suggest that at least for the years 2002-2009 which had slightly lower than average releases, it may be possible to reverse the long-term erosional trend that began when Glen Canyon Dam was completed in 1963. The only way the trend could actually be reversed, as opposed to halted, is to actively incorporate tributary-supplied sand into the active channel sediment. Thus the sustainability of current flood practices can be evaluated based on the effectiveness with which tributary-derived sediment is used to rebuild sandbars as recorded in the composition of HFE deposits, which is the objective of this study. As "sand", defined as grains with diameter 0.063-2mm, is the dominant size material with which sandbars are built (Rubin et al., 1998), discussion henceforth will exclude the finer silt and clay grain sizes (<0.063mm).

Study Setting:

As previously discussed, the only major sediment supplying-tributary for Marble Canyon is the Paria River (Fig. 1). Topping and others (2000a) estimate that in the pre-dam era, approximately 22.8 ± 1.2 million Mega grams (Mg) of sand were delivered to Marble Canyon from the Upper Colorado River basin through Glen Canyon; approximately 1.5 ± 0.3 million Mg sand were delivered by the tributary Paria River which joins the Colorado River at RM 0.9 (Lee's Ferry is RM 0). Since the dam's closure, the only sources of sediment to Marble Canyon

are the Paria River, delivering an estimated 712,000 Mg sand (based on the years 2001-2013) and minor tributary canyons supplying an estimated 72,000 t sand for the same years (Griffiths and Topping, 2015). This means that while the Paria River supplied only ~6.2% of the pre-dam sand supply to Marble Canyon, it now supplies over 90% of the total available sand. This Paria-derived sediment is typically delivered to the main stem Colorado River during the monsoon season of late summer, during flash floods triggered by intense rainfall. A sediment budget model designed by Wright and others (2010) determines the magnitude and duration of a potential HFE, aiming to maximize sand storage in Marble Canyon and minimize excessive transport out of Grand Canyon. As sand from the Paria River is the only major, reliable sediment source for Marble Canyon, the effectiveness with which it is utilized during floods via incorporation into the active sediment layer and deposited into sandbars ultimately determines the plausibility of reversing the decades long erosional patterns and thus describes the sustainability of current management practices.

Study Objectives and Hypothesis:

Assuming that the initial composition of Paria and Upper Basin sand in pre-dam sandbars was proportional to the amount of sand each source supplied, Marble Canyon sandbars likely relied on Paria-supplied sand for only about 6% of their total mass. Now, as the Paria supplies the only reliable, major sediment delivery to Marble Canyon, it is crucial that HFEs use this sand specifically to build sandbars, rather than reworking the finite supply of relict pre-dam sand only. Sediment budgets and analyses of sediment storage suggest an overall (multi-year) increase in sediment supply in Marble Canyon, requiring retention of tributary-supplied to some degree, though total storage in Marble Canyon does decrease during floods (Grams et al., 2013; Mueller et al., 2014). Sustaining this overall increase in sediment supply requires incorporation of

tributary-supplied sediment, a process that can be evaluated by determining the relative concentration of Paria-derived sediment to relict, pre-dam sand in Marble Canyon HFE deposits.

This study uses a geochemically-based sediment fingerprint approach to quantitatively determine the proportion of Paria-derived and pre-dam sand in Marble Canyon HFE deposits. Takesue and others (2004) conducted a related study, investigating minor tributary inputs to sandbars. Similar to their approach, we use elemental composition to distinguish sand from each source population (Paria River and a proxy for pre-dam sediment, see Methods for details). These end member compositions are compared to data for Marble Canyon HFE deposits to determine the relative source contribution (Paria versus relict Colorado River) to the sandbars.

A geochemically-based fingerprint takes advantage of the difference in watershed lithologies for the two source basins. While the Paria River watershed primarily drains Mesozoic sedimentary rocks, many tributaries to the Upper Colorado River have their headwaters in Pre-Cambrian igneous and metamorphic rocks characteristic of Rocky Mountain uplifts (Fig. 4). The varying mineralogic assemblages of sediment derived from these different lithologies is reflected in their elemental composition and is measurable by x-ray fluorescence (XRF) (Klages and Hsieh, 1975; Gingele and Dekker, 2005). We hypothesize that this fingerprint can 1) be used as the basis for a multivariate signal capable of differentiating source populations of sand, which can 2) determine the relative source contribution to Marble Canyon HFE deposits in a sediment mixing model.

Furthermore, differential weathering rates and styles between minerals will result in variable mineralogic compositions for each source that are unique as a function of grainsize. Thus individual fingerprints, unique to each of the six half-phi grain size fractions used in this study, should be evident and can be used to create a more robust analysis than bulk-sand

compositions would yield. The results of this mixing model contribute to the current knowledge and theories determined by GCMRC studies about sediment mixing and transport within Marble Canyon, and will additionally give insight into the overall sustainability of HFEs as a sandbar maintenance practice.

REFERENCES

Beus, S.S., C.C. Avery, L.E. Stevens, M.A. Kaplinski, and B.L.Cluer, 1992, The influence of variable discharge regimes on Colorado River sand bars below Glen Canyon Dam, *in* The Influence of Variable Discharge Regimes on Colorado River Sand Bars below Glen Canyon Dam, ed. S.S. Beus and C.C. Avery, Final Rept. to Glen Canyon Environ. Studies, N. Ariz. Univ., Flagstaff, AZ.

Department of the Interior, 2011, Environmental Assessment – Development and Implementation of a Protocol for High-Flow Experimental Releases from Glen Canyon Dam, Arizona, 2011 through 2020: Washington, D.C., Office of the Secretary of the Interior, Bureau of Reclamation, 546 p.

Dolan, R., Howard, A., and Gallenson, A., 1974, Man's impact on the Colorado River in the Grand Canyon: American Scientist, v. 62, pp. 392-401

Gingele, F. X. and Deckker, P. DE., 2005, Clay mineral, geochemical, and Sr-Nd isotopic fingerprinting of sediments in the Murray-Darling fluvial system, southeast Australia: Australian Journal of Earth Sciences, 2005, v. 52, pp. 965-974.

Graf, W. L., 2006, Downstream hydrologic and geomorphic effects of large dams on American rivers: Geomorphology, 79, pp. 336-360.

Grams, P. E., Topping, D. J., Schmidt, J. C., Hazel et al., J. E., Kaplinski, M., 2013, Linking Morphodynamic response with sediment mass balance on the Colorado River in Marble Canyon: Issues of scale, geomorphic setting, and sampling design: Journal of Geophysical Research: Earth Surface, v. 118, pp. 361-381.

Grams, P., Schmidt, J., Topping, D., 2007, The rate and pattern of bed incision and bank adjustment on the Colorado River in Glen Canyon downstream from Glen Canyon Dam, 1956-2000: GSA Bulletin, v. 119, no. 5/6, pp. 556-575.

Griffiths, R., E., Topping, D. J., 2015, Inaccuracies in sediment budgets arising from estimations of tributary sediment inputs: an example from a monitoring network on the Southern Colorado Plateau, in Technical Papers, 3rd Joint Federal Sedimentation and Hydrology Interagency Conference, Reno, NV, April 19-23, 12p.

Hazel, J. E., Kaplinski, M., Parnell, R., Manone, M., Dale, A., 1999, Topographic and Bathymetric Changes at Thirty-Three Long-Term Study Sites, *in* Webb, R. H., Schmidt, J. C.,

Marzolf, G. R., Valdez, R. A., eds. The Controlled Flood in Grand Canyon, American Geophysical Union Geophysical Monograph 110, Washington, D. C., USA, p. 161-184.

Hazel, J.E., Jr., Grams, P.E., Schmidt, J.C., and Kaplinski, Matt, 2010, Sandbar response in Marble and Grand Canyons, Arizona, following the 2008 high-flow experiment on the Colorado River: U.S. Geological Survey Scientific Investigations Report 2010–5015, 52 p.

Howard, Alan, and Dolan Robert, 1981, Geomorphology of the Colorado River in the Grand Canyon: The Journal of Geology, v. 89, no. 3, p. 269–298, doi: 10.1086/628592.

Klages, M. G., Hsieh, Y. P., 1975, Suspended solids carried by the Galatin River of Southwestern Montana: II. Using mineralogy for inferring sources. Journal of Environmental Quality, v. 4, pp. 68-73.

Lane, E.W., 1955, The importance of fluvial morphology in hydraulic engineering: Proceedings of the American Society of Civil Engineers, v. 81, paper 745, p. 1–17.

Laursen, E. M., S. Ince, and J. Pollack, 1976, On sediment transport through Grand Canyon, paper presented at Third Federal Interagency Sedimentation Conference, Water Resource Council, Denver, Colorado.

Magilligan, F. J., Nislow, K. H., 2005, Changes in hydrologic regime by dams: Geomorphology, 71, p. 61-78.

Mueller, E. R., Grams, P. E., Schmidt, J. C., Hazel, J. E., Alexander, J. S., Kaplinski, M., 2014, The influence of controlled floods on fine sediment storage in debris fan-affected canyon of the Colorado River basin: Geomorphology, 226, p. 65-75.

Petts, G. E., 1980, Long-term consequences of upstream impoundment: Environmental Conservation, v. 7, no. 4, p. 325-332

Petts, G. E., and Gurnell, A. M., 2005, Dams and geomorphology: Research progress and future directions: Geomorphology, no. 71, p. 27-47.

Randle, T.J., and Pemberton, E.L., 1987, Results and analysis of STARS (Sediment Transport and River Simulation model) modeling efforts of the Colorado River in Grand Canyon—Final report: Salt Lake City, Utah, submitted to Bureau of Reclamation, Glen Canyon Environmental Studies, 182 p. (Available from National Technical Information Service, PB88-183421.)

Richter, B.D., Baumgartner, J.V., Powell, J., Braun, D.P., 1996. A method for assessing hydrologic alteration within ecosystems. Conservation Biology 10 (4), 1163–1174.

Rubin, D.M., 2002, Recent Sediment Studies Refute Glen Canyon Dam Hypothesis: Eos, v. 83, No. 25, pp. 273, 277-78.

Rubin, D.M., Nelson, J.M., and Topping, D.J., 1998, Relation of inversely graded deposits to suspended-sediment grain-size evolution during the 1996 flood experiment in Grand Canyon:

Geology, v. 26, no. 2, p. 99–102, accessed December 29, 2009, at http://geology.gsapubs.org/content/26/2/99.

Rubin, D.M., Nelson, J.M., and Topping, D.J., 1998, Relation of inversely graded deposits to suspended-sediment grain-size evolution during the 1996 flood experiment in Grand Canyon: Geology, v. 26, no. 2, p. 99–102, accessed December 29, 2009, at http://geology.gsapubs.org/content/26/2/99.

Schmidt, J. C., 1999, Summary and synthesis of geomorphic studies conducted during the 1996 controlled flood in Grand Canyon, *in* Webb, R. H., Schmidt, J. C., Marzolf, G. R., Valdez, R. A., eds. The Controlled Flood in Grand Canyon, American Geophysical Union Geophysical Monograph 110, Washington, D. C., USA, p. 329-341.

Schmidt, J. C., Grams, P. E., Leschin, M. F.,1999, Variation in the Magnitude and Style of Deposition and Erosion in Three Long (8-12 km) Reaches as Determined by Photographic Analysis, *in* Webb, R. H., Schmidt, J. C., Marzolf, G. R., Valdez, R. A., eds. The Controlled Flood in Grand Canyon, American Geophysical Union Geophysical Monograph 110, Washington, D. C., USA, p. 329-341.

Schmidt, J.C., and Grams, P.E., 2011a, The high flows—Physical science results, *in* Melis, T.S., ed., Effects of three high-flow experiments on the Colorado River ecosystem downstream from Glen Canyon Dam, Arizona: U.S. Geological Survey Circular 1366, p. 53–91.

Schmidt, J.C., and Grams, P.E., 2011b, Understanding Physical Processes of the Colorado River, *in* Melis, T.S., ed., Effects of three high-flow experiments on the Colorado River ecosystem downstream from Glen Canyon Dam, Arizona: U.S. Geological Survey Circular 1366, p. 53–91.

Schmidt, J.C., and Wilcock, P.R., 2008, Metrics for assessing the downstream effects of dams: Water Resources Research, v. 44, no. W04404, p. 1–19, doi:10.1029/2006WR005092

Schmit, L., Gloss, S., Updike, C., 2005, Overview, *in* Gloss, S., Lovich, J. E., Melis, T. S., 2005, The state of the Colorado River Ecosystem in Grand Canyon: A report of the Grand Canyon Monitoring and Research Center 1991-2004: USGS Circular 1282, pp. 1-16.

Syvitski, J.P.M., Vorosmarty, C.J., Kettner, A.J., Green, P., 2005. Impact of humans on the flux of terrestrial sediment to the global coastal oceans: Science, v. 308, pp. 376-370.

Takesue, R.K., Rubin, D.M., Grams, P.E., 2014, Assessing erosion and re-deposition of relic (pre-dam) sand in modern Colorado River sandbars from geochemical tracers: Abstract 301-4 presented at 2014 Geological Society of America Annual Meeting, Vancouver, British Columbia, 19-22 October.

Topping, D. J., Rubin, D., Vierra, L., 2000a, Colorado River sediment transport: pt. 1: natural sediment supply limitation and the influence of Glen Canyon Dam: Water Resources Research, v. 36, p. 515-542.

Topping, D. J., Rubin, D. M., Nelson, J. M., Kinzel, P. J., Corson, I. C., 2000b, Colorado River sediment transport: 2. Systematic Bed-elevation and grain-size effects of sand supply limitation: Water Resources Research, v. 36, no. 2, pp. 543-570.

Topping, D., Schmidt, J., Vierra, L., 2003, Computation and analysis of the instantaneous-discharge record for the Colorado River at Lee's Ferry, Arizona- May 8, 1921, through September 30, 2000: US Geological Survey Professional Paper 1677, 118 p.

Topping, D.J., Rubin, D.M., Grams, P.E., Griffiths, R.E., Sabol, T.A., Voichick, Nicholas, Tusso, R.B., Vanaman, K.M., and McDonald, R.R., 2010, Sediment transport during three controlled-flood experiments on the Colorado River downstream from Glen Canyon Dam, with implications for eddy-sandbar deposition in Grand Canyon National Park: U.S. Geological Survey Open-File Report 2010–1128, 111 p. (Also available at *http://pubs.usgs.gov/of/2010/1128/*.)

U.S. Department of the Interior, 1996, Record of Decision, Operation of Glen Canyon Dam—Final Environmental Impact Statement: Washington, D.C., Office of the Secretary of the Interior, Bureau of Reclamation, 15 p.

Webb, R. H., Hereford, R., McAbe, G. J., 2005, Climatic Fluctuations, Drought, and Flow in the Colorado River, *in* Gloss, S., Lovich, J. E., Melis, T. S., 2005, The state of the Colorado River Ecosystem in Grand Canyon: A report of the Grand Canyon Monitoring and Research Center 1991-2004: USGS Circular 1282, DOI, pp. 57-68.

Wiele, S.M., Andrews, E.D., and Griffin, E.R., 1999, The effect of sand concentration on depositional rate, magnitude, and location in the Colorado River below the Little Colorado River, *in* Webb, R.H., Schmidt, J.C., Marzolf, G.R., and Valdez, R.A., eds., The controlled flood in Grand Canyon: Washington, D.C., American Geophysical Union, Geophysical Monograph Series, v. 110, p. 131–145.

Williams, G.P., and Wolman, M.G., 1984, Downstream effects of dams on alluvial rivers: U.S. Geological Survey Professional Paper 1286, 83 p.

Wright, S. A., Melis, T. S., Topping, D. J., Rubin, D. M., 2005, Influence of Glen Canyon Dam Operations on Downstream Sand Resources of the Colorado River in Grand Canyon, *in* Gloss, S., Lovich, J. E., Melis, T. S., 2005, The state of the Colorado River Ecosystem in Grand Canyon: A report of the Grand Canyon Monitoring and Research Center 1991-2004: USGS Circular 1282, DOI, pp. 17-32.

Wright, S. A., Topping, D. J., Rubin, D. M., Melis, T. S., 2010, An approach for modeling sediment budgets in supply-limited rivers: Water Resources Research, v. 46, 18 p.

CHAPTER 2: METHODS

Sediment Mixing Models

Sediment fingerprinting is a tool for understanding sediment dynamics in fluvial systems. It works on the assumptions that 1) sediment from various locations or source types within a watershed can be distinguished from one another with chemical and/or physical properties, and 2) that those properties can be used to determine, either qualitatively or quantitatively, the sources of sediment to a downstream reach (Walling et al., 1999, Koiter, et al., 2013). Since the 1970s, sediment fingerprint studies have grown both in popularity and complexity, evolving with technological advances in methods for identifying and measuring different types of properties, but also mixing model computing capabilities (Walling, 2005, 2013; Krishnappan, 2009; Gellis and Walling, 2011; Mukundan et al., 2012; Owens et al., 2016).

As one of the most fundamental ways of describing sediment composition, tracers based in mineralogy or a mix of mineralogy and corresponding elemental data were the basis of the earliest fingerprinting studies (Klages and Hseih, 1975; Wall and Wilding, 1976) and are still used in modern studies (Caitcheon et al., 2006). Today, tracer options have expanded greatly to include magnetism, radionuclides, biological indicators such as pollen and enzymes, stable isotopes and trace elements, and even color based and spectral properties (Wasson et al., 2002; Gellis et al, 2009; Brown et al., 2008; Nosrati et al., 2011; Papanicolaou et al., 2003; Collins et al., 2013a; Hewson et al., 2012; Poulenard et al., 2009).

With such an increased number of fingerprint property options, it is important and can be difficult to choose the most appropriate and effective tracers for the application at hand (Laceby et al., 2015). In studies where multiple tracer options were tested and compared, there was no

single tracer type that consistently emerged as superior to the others (Motha et al, 2002; Nosrati et al., 2011; Evrard et al., 2013). The variability between study areas, types, and applications both necessitates and resists a standardized procedure on fingerprint property selection, which several researchers have begun to develop (Collins and Walling, 2002; Collins et al., 2013; Krishnappan, 2009). Ultimately, tracer selection is dependent on the study goals, geologic setting, and analysis resources (Walling, 2013).

Aside from expanded choices for tracer properties, the methods by which sediment fingerprinting mixing models are calculated have evolved and become far more complex with technological advancement. The incorporation of linear mixing models into sediment fingerprinting studies allowed results to go beyond simply confirming sediment sources, and instead estimating the relative proportion of various sources within the mixed sediment population (Walling, 2013). As each linear mixing model could only utilize data from one tracer, fingerprinting studies with multiple tracers utilized optimization functions that simultaneously solved multiple individual linear mixing models individual each tracer (Yu and Oldfield, 1989; Walling et al., 1993). Issues with uncertainty eventually led to the incorporation of Monte Carlo methods where many iterations of these optimization functions generated a distribution of values from which relative sediment contributions and confidence limits could be determined (Krause et al., 2003; Collins et al., 2010; Devereux et al., 2010). In these Monte Carlo approaches, data were typically represented in normal distributions, though some researchers explored and advocated the use of non-normal distributions where appropriate (Devereux, 2010; Krause et al., 2003; Olley et al., 2013). Bayesian methods have since become increasingly popular, in part due to a relatively new ease of computation but also to recognition of their strengths and advantages

over non-Bayesian models (O'Hagan and Luce, 2003; Parnell et al., 2013; Butman et al., 2014; Blake et al., 2016; Owens et al., 2016).

As these methods evolve and the utility of fingerprinting studies increases, the applications of such projects are shifting from pure research incentives to supplementing and informing management practices (Gellis and Walling, 2011; Mukundan et al., 2012; Owens et al., 2016). Many studies occur in settings where undesirably high upstream sediment fluxes act as pollutants in fluvial systems, contribute to habitat degradation via high turbidity, or reduce reservoir storage capacity (Collins et al., 2011; Larsen et al., 2010). Managers often use fingerprinting studies to identify sediment sources with high erosion and sediment contribution rates when determining where restoration or prevention measures should be focused, though they can also be used to evaluate the effectiveness of such actions (Walling, 2005; Minella et al., 2008, 2009; Brown et al., 2009; Davis and Fox, 2009; Koiter et al., 2013; Olley et al., 2013). Fingerprinting studies can be used to constrain more than just the influx terms of sediment budgets as well, and many authors have advocated its use in understanding sediment storage, transport dynamics, and residence times (Wethered et al., 2015; Gellis and Walling, 2011; Smith et al., 2011; Guzman et al., 2013), in addition to a much wider range of other applications (Owens et al., 2016). This study documents a relatively novel application of sediment fingerprinting: while, similar to other studies, it evaluates restorative management efforts, these efforts are focused on increasing downstream aggradation rather than preventing upstream erosion, and the results are used to ultimately determine the overall sustainability of the management practices. The most closely related study to date evaluated sediment sources responsible for restorative aggradation in coastal salt marshes with a fingerprinting study based in environmental magnetism (Rotman et al., 2008).

The objective of this project is to determine the contribution of Paria-derived sediment to restored Marble Canyon sandbars through use of sediment fingerprinting, using the effectiveness with which the only renewable source of sand is utilized in HFE deposits to evaluate the overall sustainability of current sandbar maintenance practices. Principal components of elemental data measured by x-ray fluorescence (XRF) are used in a Bayesian mixing model to determine the source contribution to HFE deposits at fourteen sites deposited during two flood events. The primary advantages of Bayesian methods that apply to this project are: ability to recognize source properties as random variables due to incomplete knowledge, include and propagate property uncertainty for all sand populations throughout the model, and the ability utilize raw data instead of loading a generalized distribution (Caitcheon et al., 2006; Davis and Fox, 2009; Barthod et al., 2015; Owens et al., 2016; Stock and Semmens, 2016). The mixing model used in this study was developed and implemented in MixSIAR (Stock and Semmens, 2013), which runs in R (R Core Team, 2016) using JAGS for Markov Chain Monte Carlo (MCMC) simulation (Plummer, 2016). MixSIAR also provides a series of diagnostic tests that allow the user to evaluate how successful the mixing model was, largely determined by chain convergence (Stock and Semmens, 2016). MCMC is discussed in greater detail below, and a summary of diagnostics is available by request.

Endmember Characterization:

The mixing model in this study aims to determine the relative contributions of Paria and relict, pre-dam sand stored in the channel to Marble Canyon HFE deposits. While Paria-derived sand is readily available, is impossible to confidently sample from relict pre-dam sand in the main-stem Colorado River in Marble Canyon. For this reason, terraces in the lower Glen Canyon reach of the Colorado River below Glen Canyon Dam but above the Paria River Confluence

were used as a proxy for pre-dam sediment previously delivered from the Upper Colorado River Basin to Marble Canyon. All of the sampled terraces were above the first significant gully in Glen Canyon in order to preserve the original composition of upper basin sediment and not over-represent sediment from the Navajo Sandstone which forms the canyon walls of Glen Canyon. The terraces themselves typically rose 3-5m above and were stratigraphically continuous down to the current river level. Trenches dug into the basal sections of these terrace deposits revealed the internal stratigraphic organization which served as guideline for sample locations; the same methods are described in more detail, below, for Marble Canyon HFE deposits. Samples were not taken from above the typical post-dam high water line to avoid the influence of diagenetic processes (Koiter et al., 2013), as the terraces were often very well consolidated and cemented to a higher degree than active fluvial sandbars.

Suspended sediment concentration (SSC) and discharge on the Paria River is monitored at USGS station 9382000 (Fig. 3a, b) with suspended sediment samples collected by an automatic sampler at various times throughout the duration of monsoon season flash floods. As the source of sediment transported during floods can shift over the duration of the storm, multiple samples were taken during each flood on the Paria River (Fig. 3a, b; Slattery et al., 2000; Wilson et al., 2008). The sampler is also near the confluence of the Paria and Colorado Rivers, below the input of all major tributary streams, making samples from this location representative of the entire watershed. Collins and others (1998) and Walling and others (1999) document the importance of seasonal variance in suspended sediment and the importance of sampling throughout the year to accurately represent the sediment population. Because the Paria River delivers sediment almost solely during monsoon season (Fig. 3c), samples from mid-summer through fall are considered be representative of the annual Paria load. Concerns over

discrepancies between the tracer properties of non-eroded sediment sources and those of the suspended sediment they generate do not apply here, as not only the Paria-derived sediment but all sediment used in this study was either currently or recently suspended at the time of sampling (Walling et al., 2005; Collins et al., 2010). A total of 44 suspended sediment samples were chosen to characterize Paria River sediment, delivered by monsoon floods before both the 2013 and 2014 HFEs. Samples used in this study were selected from those available based on the behavior of both discharge and SSC, choosing samples taken during the rising limb, peak, and falling limb of both floods and sediment pulses (Fig. 3 a, b). Multi-day floods often had several intermediate peaks within them and were included in the sampling scheme.

A total of 20 Marble Canyon HFE deposits were sampled at 14 sandbars, twelve of which are long-term study sites for Northern Arizona University Sandbar Studies, with repeat sets of samples from both the 2013 and 2014 HFE deposits at six locations (Fig. 5a). At each bar, a trench was dug to reveal the internal stratigraphy of the deposit, as sedimentary structures within the deposits responded to changing hydrologic and suspended sediment conditions throughout the duration of deposition. Typical bar deposits were similar to those reported by Rubin et al., 1998 and exhibited some of the signs of suspended sediment limitation addressed by Topping and others (2000a): coarsening upwards with clay-rich basal layer, main body of (typically) climbing ripples, and uppermost section of planar bedding (Fig. 5b). Deposit stratigraphy was also used to interpret the year of deposition, only taking samples the most recent HFE deposits. Table 2 contains the year of deposition, location, deposit height, and number of samples per deposit for all HFE deposits used in this study.

Sample Processing

Standard pre-processing prior to testing consisted of sieving into half-phi grain size fractions, washing in deionized water, and then drying in an oven prior to testing with XRF. In contrast to the previously mentioned study by Takesue (2014) where the 0.063-0.250 mm fraction of sand was analyzed in bulk via total decomposition with ICP-MS and ICP-AES, sand in this study was sieved into half-phi grain size fractions prior to testing. Taking advantage of the differential breakdown of different families of minerals served as the motivation for this step, intending to utilize any subtle, grain size-dependent differences in mineralogic composition between the two endmember sand sources that would otherwise be buried in a bulk-decomposition analysis. Additionally, sieving prevented the need for grain size correction factors, which have been shown to produce erroneous results or bias (Smith and Blake, 2015; Kraushaar et al., 2015). Following sieving, the samples were washed in deionized water: stirred vigorously to dislodge and break up any clay aggregates or grain coatings, and decanted while still in suspension. Dispersion agents were foregone to avoid leaving a chemical trace capable of skewing XRF readings. Samples were then dried in an oven at approximately 250° F, and re-packaged into 1.5 x 1.5 inch, 2 mil, polyethylene film bags for testing. Samples were tested directly through these bags; each bag contained sand from one grain size fraction of one sample of either Paria suspended sediment, pre-dam terrace from Glen Canyon, or Marble Canyon HFE deposit. Grain size fractions tested were those described by Rubin (1998) as the primary bar-building sizes (0.063-0.250 mm), as well as additional, coarser, sizes for which there was a sufficient *n* for both endmembers (0.063 – 0.500 mm, Table 3).

X-ray Florescence (XRF)

X-ray florescence, or XRF, is a technique used to measure the elemental composition of a material. High-energy x-rays are directed at the sample, where electrons within the sample material are excited to an elevated shell within the atom. As the electrons fall back to their original shell, they emit energy in the form of an x-ray whose frequency is characteristic of the element; these frequencies are dependent on which shells the electron fall from/to. The XRF detector measures the abundance of each unique x-ray to determine the concentration of that element within the sample. The Niton XLT3 portable XRF used in this study emits a 50 kV x-ray, and can detect x-rays characteristic to over thirty-five major and trace elements. It is important to note that the elemental composition data measured by the XRF and reported here is non-standardized: for each run, all reported elemental concentrations are proportionally correct relative to each other but cannot be substituted for absolute values due to factors such as grain orientation, sample density and the resulting matrix effects and spectral interference (Sherman, 1955; Castro et al., 2008; Yalcin et al., 2008). Other studies that have employed the use of XRF include: Gingele and Dekker (2005), Melquiades and others (2013), Hughes and others (2010), and Caitcheon and others (2006).

Several factors were considered when designing the XRF test protocol for this study, including: which elements to test for, test duration, sample heterogeneity, and sample mass. Of the four filters with which the XRF is equipped (each specialized to detect a certain suite of elements), the Main (Magnesium through Molybdenum), Low (Titanium through Chromium), and Light (Carbon through Chlorine) filters were used to measure the concentration of over 35 elements in the samples. Each filter was employed for 30 seconds in each run. The 30 second duration was long enough such that measured elemental concentrations displayed in real time

during the tests had stabilized by the time each filter was finished detecting. Each individual bag was tested for a total of three 90-second runs, accounting for sample heterogeneity by repositioning the bag or disturbing the sand between each run. This was especially important for the coarser grain sizes, where the ratio of spot size to grain size was much smaller than for the finest grain sizes. The final consideration when testing the samples with XRF was sample mass, and consequently, thickness. The effects of sample thickness on XRF results was tested by repeatedly measuring individual samples with incrementally decreasing mass. Readings remained relatively constant for samples greater than approximately 0.5 g, and tended to increase dramatically with sample mass <0.5 g; individual grain size fraction samples with mass <0.5 g were thus excluded from this study.

Data Preprocessing

Of the 35+ elements reported by the XRF, eleven had measured concentrations greater than the minimum level of detection for all or nearly all samples from all three populations. (Fe, Ca, Al, Si, P, S, Cl, Ti, Rb, Sr, and Zr). Given the non-standardized nature of the data, ratios of reported element concentration must be used to compare values between samples. Thus, all possible permutations of these twelve elements, a total of 55 ratios, were calculated for each individual run (Fe/Ca, Fe/Al, etc.). Any elemental concentrations initially reported as below the level of detection were replaced with the minimum reported value for that population prior to calculating ratios. The average value of each ratio across the three runs was calculated and considered representative of that sample.

Data used in mixing models must pass two general criteria: 1) “conservativeness”, requiring that values for the mixed population are intermediate to the endmembers, and 2) the difference in values for the endmember populations must be statistically significant (Collins et

al., 1996). Following the methods outlined by Collins and others (1996) that are generally regarded as a standard statistical test for property selection, conservativeness is tested by comparing the mean values of a ratio from each of the three populations, ensuring that the value for the mixed population falls between the two endmembers. The Kruskal-Wallis H-test, a non-parametric assessment of variance (ANOVA), is then used to evaluate the difference between the two endmember populations; this test was chosen over other ANOVA tests as it was most appropriate for the non-normally distributed data in this study. This process determined the suite of ratios unique to each grain size eligible for consolidation into a multivariate metric for use in the mixing model, successfully exploiting any grain size-dependent differences in mineralogic composition among the different size fractions.

Principal Components Analysis

Melquiades and others (2013) demonstrated the utility of Principal Components Analysis (PCA) to create multivariate metrics capable of distinguishing different populations of sediment based on XRF data. PCA works to consolidate the original input variables defining your endmembers, variables that often have numerous and complex relationships with each other, into composite independent variables with covariances of zero. Each principal component is a linear combination of the original variables, and is described by an axis (PC1, PC2, etc.) throughout a multi-dimensional cloud of the data; each axis is orthogonal to the previous one(s). The resulting Principal Components (PCs) are ordered variables, with the first PC capable of explaining the highest proportion of the total variance in the original data and each successive PC explaining decreasingly less of the total variance (Melquiades et al., 2013). While PCA returns the same number of PCs as original variables, the first two or three often explain a sufficient amount of the original variance and are thus the only PCs used in analyses. The value of using PCs as the

multivariate metric for a mixing model is their ability to represent the variability of all available data in each of the three populations (two endmembers and mixed). This study ran individual PC analyses on the Glen Canyon and Paria samples from each of the six grain size fractions. Each PCA utilized a correlation matrix to determine the PC axes (and related linear transformations for each original ratio to give the PC values), which essentially equalizes the ability of all possible ratios to influence PC values. The alternative to using a correlation matrix is a covariance matrix, which considers the covariance between the original variables (eligible ratios) as opposed to the correlation. In this study, using the covariance matrix would allow the ratios with a larger magnitude range to have a much higher influence over final PC values than those with a small range. Using a correlation matrix to compute PCs avoids this undesired effect by essentially normalizing the values for all eligible ratios before determining the loadings that define the linear transformations used to calculate PC values.

Raw values for PC1 and PC2, which explained approximately 60-70% of the total original endmember variance for all grain sizes (Table 4), were used in the mixing model. The third PC was not utilized in the mixing model due to its inability to distinguish the two endmember populations. For all grainsizes, PC1 has the stronger control on differentiating the Glen Canyon and Paria sand, and is the primary axis along which Marble Canyon sand falls intermediate to the two endmembers (Fig. 6a). Loadings plots (Fig. 6b) indicate which elemental ratios influence PC1 and PC2 which gives insight into how different minerals present in the two watersheds are used in the fingerprints. Additionally, the ratios with the heaviest loadings on PC1 and PC2 vary for each grain size fraction, thus confirming the utility of analyzing each fraction separately. In the 63-90 fraction, many of the ratios weighing most heavily on PC1 involve Ti, with Ti in the denominator and elements such as K and Si in the numerator on the

positive side of the x-axis. This means that as these ratios increase, as Ti levels decrease and Si and K levels increase, PC1 values are become more positive which is characteristic of Paria-derived sand; this trend likely reflects differences in the abundance of biotite and amphiboles (more likely to occur in Glen Canyon sand) versus K-feldspar and quartz (more abundant in Paria sand). In a similar fashion, ratios in the 90-125 μm such as Fe/S, Rb/Sr, K/Sr, and Ca/Ti suggest that different abundances of iron oxides and biotite vs. feldspars are likely responsible for the distinction of Glen Canyon and Paria sand along PC1. The 125-180 μm fraction appears to be largely influenced by the presence of zircons in the Glen Canyon sand, as shown by the ratios with Zr in the denominator on the Paria side: as Zr levels increase, the value for those ratios decreases thus becoming more like Glen Canyon sand. PC1 in the three coarsest fractions is consistently influenced by ratios with Rb and Sr, and Fe has a strong influence on PC1 in the two coarsest fractions. These ratios likely reflect higher abundances of biotite and iron oxides in the Glen Canyon sand, and more quartz and feldspars in the Paria sand for these fractions.

MixSIAR

The mixing model used in this study is 'MixSIAR', a package for the R environment that designs Bayesian mixing models based on the given data and user options, and is run using the 'JAGS' R package (Stock and Semmens, 2013; Plummer, 2016). Though originally developed for diet analyses in ecological applications, the authors explicitly state its potential for other applications and has been used to analyze suspended sediment mixing before (Nakayama, 2014). Strengths of MixSIAR included its ability to represent non-normal and complex data, the ability to tailor the model design to the data used and model purpose, and providing thorough diagnostics concerning the model's accuracy. The options for model customization used in this study are: 1) choosing to use any number of tracers, 2) choosing a "residual only" or "residual

and process" error structure, and 3) the ability to use a non-informative, or generalist, prior. As previously mentioned, PC1 and PC2 were used to describe the source and mixed populations in this study; a separate mixing model was run for each grain size fraction. For each of the six grain size fractions, all available PC1 and 2data were used to characterize the three populations in the model. The *n* for each population in each grain size fraction is summarized in Table 3; Marble Canyon HFE deposits are subdivided by site. A "residual only" error structure was chosen, as process-based error structures are appropriate for diet based data but not geologic composition data (Stock and Semmens, 2016). Given the absence of any definitive prior knowledge on the contribution of Paria-derived sediment to Marble Canyon HFEs, an uninformative prior was used.

When running the model, JAGS uses a technique called MCMC, or Markov Chain Monte Carlo, to determine the most likely proportion of the two source populations in the mixed Marble Canyon populations, based on their composition as described by PC1 and PC2. This process takes place in a multi-dimensional parameter space where the values in that space represent the possible proportions of Glen Canyon and Paria contributions to each of the sampled Marble Canyon HFE deposits. In MCMC, an individual "chain" will wander through the parameter sampling parameter values that have a high likelihood of producing the observed tracer data for Marble Canyon samples. The ability of PC1 and PC2 to distinguish the two sources is incorporated into the model via their respective representation of variability in the source and mixture tracer data; value weightings describing these abilities are unnecessary, thus avoiding any inaccuracies or bias they might introduce (Laceby and Olley, 2015). Most models, this one included, employ multiple chains that start at different positions n parameter space and must all converge on the same final distribution of parameter values. Test designs must comprise a

sufficiently large number of MCMC iterations to reach chain convergence, though additional iterations do not increase posterior accuracy. Trace plots to evaluate the convergence of all chains are one of the many diagnostics available with MixSIAR that evaluate the generality and accuracy of the test. MCMC also makes use of the full distribution of values for all three populations, and provides the means for incorporating and propagating uncertainty throughout the entire model (Davis and Fox, 2009; Fox and Papanicolaou, 2009; Cooper et al., 2015). The initial steps of MCMC wandering have not had time to reach parameter combinations with high likelihoods, and are thus discarded; these initial estimates are the "burn-in". Additionally, because each step of an MCMC chain is not independent from the previous step, "thinning" is used to select a subset of samples taken at a regular interval along the chain. This study used the "normal" test setting in MixSIAR, which uses a total of 100,000 MCMC iterations for three chains, the first 50,000 of which are the burn-in, with a thinning interval of 50: using 1 in every 50 iterations from all three chains. These thinned samples from the converged chains then collectively represent the posterior distribution for each estimated parameter, which in this case is the proportion of sediment originating from each source estimated for each Marble Canyon HFE deposit. The reported Apparent Paria Percentage (APP) and uncertainty are derived from the mean and standard deviation of these posterior distributions. Please see the supplementary document, available online, for complete mixing model diagnostics.

REFERENCES

Barthod, L.R.M., Liu, K., Lobb, D.A., Owens, P.N., Martinez-Carreras, N., Koiter, A.J., Petticrew, E.L.,McCullough, G.K., Liu, C., Gaspar, L., 2015, Selecting color-based tracers and classifying sediment sources in the assessment of sediment dynamics using sediment source fingerprinting: Journal of Environmental Quality, v. 44, pp. 1605–1616.

Blake, W., Smith, H., Navas, A., Bode, S., Goddard, R., Kuzyk, Z., Lennard, A., Lobb, D., Owens, P., Palazon, L., Petticrew, E., Gaspar, L., Stock, B., Boeckx, P., Semmens, B., 2016, Application of hierarchical Bayesian unmixing models in river sediment source apportionment: Geophysical Research Abstracts, v. 18, EGU General Assembly, EGU2016-10043.

Brown, A. G., Carey, C., Erkens, Gilles, Fuchsm M., Hoffman, T., Macaire, J., Moldenhauer, K., Walling, D. E., 2009, From sedimentary records to sediment budgets: Multiple approaches to catchment sediment flux: Geomorphology, v. 108, pp. 35-47.

Brown, A.G., Carpenter, R.G., Walling, D.E., 2008, Monitoring the fluvial palynomorph load in a lowland temperate catchment and its relationship to suspended sediment and discharge: Hydrobiolgia, v. 607, pp. 27-44, DOI 10.1007/s10750-008-9364-6.

Butman, D. E., Wilson, H. F., Barnes, R. T., Xenopoulos, M. A., Raymond, P. A., 2014, Increased mobilization of aged carbon to rivers by human disturbance: Nature Geoscience, pp. 1-6.

Caitcheon, G., Douglas, G., Palmer, M., 2006, Sediment Source Tracing in the Lake Burragorang Catchment: SCIRO Land and Water Science Report 47/07, 29 p.

Castro, K., Pessanha, S., Proietti, N., Princi, E., Capitani, D., Carvalho, M.L., Madariaga, J.M., 2008, Noninvasive and nondestructive NMR, Raman and XRF analysis of a Blaeu coloured map from the seventeenth century: Anals of Bioanalytical Chemistry, v. 391, pp. 433–441.

Collins AL, Walling DE, Leeks GJL, 1996, Use of composite fingerprints to determine the provenance of the contemporary suspended sediment load transported by rivers: Earth Surface Processes and Landforms, v. 32, pp. 31-52.

Collins AL, Zhang Y, Duethmann D, Walling DE, Black KE, 2013, Using a novel tracing-racking framework to source fine-grained sediment loss to watercourses at catchment scale. Hydrological Processes, v. 27, pp. 959–974.

Collins AL, Zhang Y, Hickinbotham R, Bailey G, Darlington S, Grenfell SE, Evans R, Blackwell M, 2013, Contemporary fine-grained bed sediment sources across the River Wensum Demonstration Test Catchment, UK. Hydrologic Processes, v. 27, pp. 857–884.

Collins AL, Zhang Y, Walling DE, Grenfell SE, Smith P, 2010, Tracing sediment loss from eroding farm tracks using a geochemical fingerprinting procedure combining local and genetic algorithm optimization: Science of the Total Environment, v. 408, pp. 5461–5471.

Collins, A. L., Walling, D. E., 2002, Selecting fingerprint properties for discriminating potential suspended sediment sources in river basins: Journal of Hydrology, v. 261, pp. 218-244.

Collins, A.L., Walling, D.E., Leeks, G.J.L., 1998, Use of composite fingerprints to determine the provenance of the contemporary suspended sediment load transported by rivers: Earth Surface Processes and Landforms, v. 23, pp. 31-52.

Cooper, R.J., Krueger, T., Hiscock, K.M., Rawlins, B.G., 2015, High temporal resolution fluvial sediment source fingerprinting with uncertainty: a Bayesian approach: Earth Surface Processes and Landforms, v. 40, pp. 78–92.

Davis, C. M., Fox, J. F., 2009, Sediment Fingerprinting: Review of the Method and Future improvements for allocating nonpoint source pollution: Journal of Environmental Engineering, v. 135, no. 7., pp. 490-504.

Devereux OH, Prestegaard KL, Needelman BA, Gellis AC, 2010, Suspended-sediment sources in an urban watershed, Northeast Branch Anacostia River, Maryland: Hydrological Process, v. 24, pp. 1391–1403.

Evrard, O Poulenard J, Némery J, Ayrault S, Gratiot N, Duvert C, Prat C, Lefèvre I, Bonté P, Esteves M, 2013, Tracing sediment sources in a tropical highland catchment of Central Mexico by using conventional and alternative fingerprinting methods: Hydrologic Processes, v. 7, pp. 911–922.

Fox, J. F., Papanicolaou, A., N., 2008, An un-mixing model to study watershed erosion processes: Advances in Water Resources, v. 31, pp. 96-108.

Gellis AC, Hupp CR, Pavich MJ, Landwehr JM, Banks WSL, Hubbard BE, Langland J, Ritchie JC, Reuter JM, 2009, Sources, transport, and storage of sediment at selected sites in the Chesapeake Bay Watershed: US Geological Survey Scientific Investigations Report 2008–5186, 110 p.

Gellis, A., and Walling, D. E., 2011, Sediment Source Fingerprint (Tracing) and Sediment Budgets as Tools in Targeting River and Watershed Restoration Programs: Geophysical Monograph Series 194, pp. 263-291

Gingele, F. X. and Deckker, P. DE., 2005, Clay mineral, geochemical, and Sr-Nd isotopic fingerprinting of sediments in the Murray-Darling fluvial system, southeast Australia: Australian Journal of Earth Sciences, 2005, v. 52, pp. 965-974.

Hewson RD, Cudahy TJ, Jones M, Thomas M, 2012, Investigations into soil composition and texture using infrared spectroscopy (2–14 μm): Applied Environmental Soil Sciences, doi:10.1155/2012/535646.

Hughes, A.O., Croke, J.C., Pietsch, T.J., Olley, J.M., 2010, Changes in the rates of floodplain and in-channel bench accretion in response to catchment disturbance, central Queensland, Australia. Geomorphology 114, 338–347.

Klages, M. G., Hsieh, Y. P., 1975, Suspended solids carried by the Galatin River of Southwestern Montana: II. Using mineralogy for inferring sources. Journal of Environmental Quality, v. 4, pp. 68-73.

Koiter, A.J., Owens, P.N., Petticrew, E.L., Lobb, D.A., 2013, The behavioural characteristics of sediment properties and their implications for sediment fingerprinting as an approach for identifying sediment sources in river basins. Earth Science Review, v. 125, pp. 24–42.

Krause AK, Franks SW, Kalma JD, Loughran RJ, Rowan JS, 2003, Multi-parameter fingerprinting of sediment deposition in a small gullied catchment in SE Australia: Catena v. 53, pp. 327–348.

Krishnappan, B. G., Chambers, P. A., Benoy, G., Culp, J., 2009, Sediment source identification: a review and a case study in some Canadian streams: Canadian Journal of Civil Engineering, v. 36, pp. 1622-1633.

Laceby, J. P., McMahon, J., Evrard, O., Olley, J., 2015, A comparison of geological and statistical approaches to element selection for sediment fingerprinting: Journal of Soils and Sediments, v. 15, pp. 2117-2131. DOI: 1 0.1007/s11368-015-1111-9.

Laceby, J.P., and Olley, J., 2015, An examination of geochemical modelling approaches to tracing sediment source incorporating distribution mixing and elemental correlations: Hydrological Processes, v. 29, pp. 1669-1685, DOI 10.1002/hyp.10287.

Larsen, M.C., Gellis, A.C., Glysson, G.D., Gray, J.R., Horowitz, A.J., 2010, Fluvial sediment in the environment: A National challenge, *in*, Proceedings of the 4th Federal Interagency Hydrologic Modeling Conference and the 9th Federal Interagency Sedimentation Conference, Las Vegas: Nevada, U.S. Geological Survey, U.S. Department of the Interior, 15p.

Melquiades FL, Andreoni LFS, Thomaz EL, 2013, Discrimination of landuse types in a catchment by energy dispersive X-ray fluorescence and principal component analysis. Applied Radioactive Isotopes, v. 77, pp. 27–31.

Minella, J. P. G., D. E. Walling, and G. H. Merten, 2008, Combining sediment source tracing techniques with traditional monitoring to assess the impact of improved land management on catchment sediment yields: Journal of Hydrology, v. 348, no. (3–4), pp. 546–563.

Minella, J. PG., Merten, G. H., Walling, D. E., Reichert, J. M., 2009, Changing sediment yield as an indicator of improved soil management practices in southern Brazil: Catena, v. 79, pp. 228-236.

Motha JA, Wallbrink PJ, Hairsone B, Grayson RB, 2002, Tracer properties of eroded sediment and source material: Hydrologic Processes, v. 16, pp. 1983–2000.

Mukundan, R., Walling, D.E., Gellis, A.C., Slattery, M.C., Radcliffe, D.E., 2012, Sediment source fingerprinting: transforming from a research tool to a management tool: Journal of the American Water Resource Association, http://dx.doi.org/10.1111/j.1752-1688.2012.00685.x.

Nakayama, K., Beitia, C., Ohtso, N., Yamasaki, S., Yasayuki, M., Yamane, M., 2014, Fingerprint methods for suspended sediment transport processes by using X-ray fluorescence analysis: Abstract H51O-0811 presented at the 2014 Fall Meeting, AGU, San Francisco, California, 15-19 December.

Nosrati K, Govers G, Ahmadi H, Sharifi F, Amoozegar MA, Merckx R, Vanmaercke M, 2011, An exploratory study on the use of enzyme activities as sediment tracers: biochemical fingerprints? International Journal of Sediment Research v. 26, pp. 136–151.

O'Hagan, A., Luce, B. R., 2003: A primer on Bayesian statistics in Health Economics and Outcomes Research: MEDTAP International, Inc.

Olley JM, Burton J, Smolders K, Pantus F, Pietsch T, 2013, The application of fallout radionuclides to determine the dominant erosion process in water supply catchments of subtropical South-east Queensland, Australia. Hydrologic Process, v. 27, pp. 885–895.

Owens, P. N., Blake, W. H., Gaspar, L., Gateuille, D., Koiter, A. J., Lobb, D. A., Petticrew, E. L., Reiffarth, D. G., Smith, H. G., Woddward, J. C., 2016, Fingerprinting and tracing the sources of soils and sediments: Earth and ocean science, geoarchaeological, forensic, and human health applications: Earth-Science Reviews, v. 162, pp. 1-23.

Papanicolaou AN, Fox JF, Marshall J, 2003, Soil fingerprinting in the Palouse basin, USA using stable carbon and nitrogen isotopes: International Journal of Sediment Research v. 18, pp. 291–297.

Parnell, A. C., Phillips, D. L., Bearhop, S., Semmens, B. X., Ward, E. J., Moore, J. W., Jackson, A. L., Grey, J., Kelly, D. J., and Inger, R., 2013, Bayesian stable isotope mixing models: Environmetrics, v. 24, no. 6, pp. 387-399.

Plummer, M., 2016, rjags: Bayesian Graphical Models using MCMC. R package version 4-6. https://CRAN.R-project.org/package=rjags.

Poulenard J, Perrette Y, Fanget B, Quetin P, Trevisan D, Dorioz JM, 2009, Infrared spectroscopy tracing of sediment sources in a small rural watershed (French Alps). Science of the Total Environment, v. 407, pp. 2808–2819.

R Core Team, 2016, R: A language and environment for statistical computing. R Foundation for Statistical Computing, Vienna, Austria. URL https://www.R-project.org/.

Rotman, R., Naylor, L., McDonnel, R., MacNiocaill, C., 2008, Sediment transport on the Freiston Shore managed realignment site: An investigation using environmental magnetism: Geomorphology, v. 100, pp. 241-255.

Rubin, D.M., Nelson, J.M., and Topping, D.J., 1998, Relation of inversely graded deposits to suspended-sediment grain-size evolution during the 1996 flood experiment in Grand Canyon: Geology, v. 26, no. 2, p. 99–102, accessed December 29, 2009, at http://geology.gsapubs.org/content/26/2/99.

Sherman, J., 1955, The theoretical derivation of fluorescent X-ray intensities from mixtures: Spectrochimica Acta, v. 7, pp. 283-306.

Smith, H.G., Blake, W.H., 2014, Sediment fingerprinting in agricultural catchments: a critical re-evaluation of source discrimination and data corrections: Geomorphology, v. 204, pp. 177–191.

Stock, B. C. and B. X. Semmens, 2013, MixSIAR GUI User Manual. Version 3.1. https://github.com/brianstock/MixSIAR/. DOI:10.5281/zenodo.47719

Stock, B.C., Semmens, B.X., 2016, Unifying error structures in commonly used biotracer mixing models: Ecology, v. 97, no. 10, pp. 2562-2569.

Takesue, R.K., Rubin, D.M., Grams, P.E., 2014, Assessing erosion and re-deposition of relic (pre-dam) sand in modern Colorado River sandbars from geochemical tracers: Abstract 301-4 presented at 2014 Geological Society of America Annual Meeting, Vancouver, British Columbia, 19-22 October.

Wall GJ, Wilding LP, 1976, Mineralogy and related parameters of fluvial suspended sediments in northwestern Ohio: Journal of Environmental Quality, no. 5, pp. 168–173.

Walling, D. E., 2005, Tracing suspended sediment sources in catchments and river systems: Science of the Total Environment, v. 344, pp. 159-184.

Walling, D. E., 2013, The evolution of sediment source fingerprinting investigations in fluvial systems: Journal of Soils and Sediments, v. 13, pp. 1658-1675.

Walling, D.E., P.N. Owens, and G.J.L. Leeks, 1999. Fingerprinting Suspended Sediment Sources in the Catchment of the River Ouse, Yorkshire, UK. Hydrological Processes 13:955-975.

Walling, D.E., Woodward, JC., Nicholas, A.P., 1993, A multi-parameter approach to fingerprinting suspended sediment sources *in* Peters, N.E., Hoehn, E., Leibundgut, C., Tase, N., Walling, D. E., (eds) Tracers in hydrology: IAHS Publication no. 215. IAHS, Wallingford, pp. 329–338.

Wasson RJ, Caitcheon G, Murray AS, McCulloch M, Quade J, 2002, Sourcing sediment using multiple tracers in the catchment of Lake Argyle, Northwestern Australia: Environmental Management, v. 29, pp. 634–646.

Wethered, A.S., Ralph, T.J., Smith, H.G., Fryirs, K.A., Heijnis, H., 2015, Quantifying fluvial (dis)connectivity in an agricultural catchment using a geomorphic approach and sediment source tracing: Journal of Soils and Sediments, v. 15, pp. 2052-2066.

Yalcin, G.M., Narin, I., Soylak, M., 2008. Multivariate analysis of heavy metal contents of sediments from Gumusler creek, Nigde, Turkey: Environmental Geology, v. 54, pp. 1155–1163.

Yu, L., Oldfield, F., 1989, A multivariate mixing model for identifying sediment sources from magnetic measurements: Quaternary Resources, v. 31, pp. 168–181.

CHAPTER 3: MANUSCRIPT

INTRODUCTION

Large dams commonly disrupt the balance of sediment supply and transport capacity of downstream fluvial systems, resulting in spatially and temporally extensive geomorphic changes to the affected channel (Williams and Wolman, 1984; Poff et al., 1997; Syvitski et al., 2005; Magilligan and Nislow, 2005, Graf et al., 2006). Depending on the magnitude and direction of changes to sediment supply and transport capacity, the sediment mass balance of downstream reaches will be pushed into either surplus or deficit, resulting in aggradation or erosion, respectively (Lane et al, 1955; Petts and Gurnell, 2005; Schmidt and Wilcock, 2008). Altering dam releases in restoration and management practices can help mitigate these effects by aiming to imitate critical components of the pre-dam flow regime such as floods. System complexity and economic or resource-related complications can make it difficult to design and implement an effective management protocol as each solution is unique to the selected system (Poff et al., 1997; Magilligan and Nislow, 2005).

One such example is in the Southwestern United States, where the 1963 completion of Glen Canyon Dam (Fig. 1) quickly induced significant geomorphic change to the downstream reaches of the Colorado River through Grand Canyon (Dolan et al., 1974). More than 20 years of management practices centered around dam-release floods address and aim to reverse a primary component of this change: the depletion of eddy sandbar deposits. This study assesses the effectiveness and sustainability of Colorado River sandbar restoration under current management practices (Department of the Interior, 1995, 1996, 2011), using quantitative sedimentological tools to understand post-dam sediment mixing and depositional processes.

The pre-dam Colorado River in Grand Canyon experienced alternating, seasonally driven, periods of sediment surplus and deficit (Topping et al., 2000). Late-summer monsoon season flash floods delivered sediment to the main channel which was then reworked during the much larger annual spring snowmelt floods. Deposits from these pre-dam spring floods coarsen upwards indicating that the fine sediment supply became limited during floods (Leopold and Maddock, 1953; Rubin et al., 1998, Topping et al., 2000). A higher degree of fine sediment supply limitation exists on the post-dam Colorado River, due to dam-induced changes to the hydrologic and sediment regimes (Topping et al., 2000). Glen Canyon Dam effectively eliminated spring snowmelt floods of the Colorado River downstream in Grand Canyon and severely dampened the magnitude of annual seasonal variability: the magnitude two-year recurrence floods was reduced by 62% whereas median flows were increased by 58% (Fig. 2, Topping et al., 2003). Sediment delivery from the upper Colorado River Basin, the primary pre-dam source of sand in the downstream Grand Canyon, is now effectively zero, and the relatively small supply of sediment previously stored in Lower Glen Canyon was depleted during a series of pulse flows in 1965 (Topping et al., 2000, Grams et al., 2007; Mueller et al., 2014). Because this incoming sediment was critical to maintaining emergent sandbars within the downstream debris fan-eddy complexes and channel margins in Marble Canyon, considerable sandbar erosion occurred in response to the greatly reduced sediment supply (Dolan et al., 1974; Schmidt and Rubin, 1995, Grams et al., 2007).

The ecological and recreational value of these sandbars placed their restoration among the top priorities of federal resource managers (Kearsely et al., 1994; Schmit et al., 2005; Schmidt and Grams, 2011a; Department of the Interior, 2011). Today, controlled floods referred to as High Flow Experiments (HFEs) are used in attempts to rebuild sandbars in the reaches of

the Colorado River downstream of Glen Canyon Dam throughout Grand Canyon (Schmit et al., 2005; U.S. Department of the Interior, 1995). To date, a total of seven HFEs (summarized in Table 1) have occurred. As part of the greater Glen Canyon Dam Adaptive Management Program (GCDAMP), scientific monitoring during and between floods is used to continually improve upon flood design and optimize the degree to which sand storage in Grand Canyon increases (U.S. Department of the Interior, 1996; Webb et al., 1999; Hazel et al., 2006, 2010; Topping et al., 2010, Melis, 2011,). The extent of eddy-sandbar deposition is ultimately a function of the suspended sediment concentration during floods, which depends on the amount of antecedent sand enrichment (ASE; tributary-supplied sediment stored in the channel prior to a flood), the areal extent of that sediment, and its grain size distribution (Wiele et al., 1999; Schmidt, 1999). In consideration of this, continuously monitored data about sediment inputs and outputs is used in a sediment routing model designed by Wright and others (2010) to determine the flood magnitude and duration necessary to maximize sediment storage during HFEs and minimize excess downstream transport (U.S. Department of the Interior, 2011). Sandbar and channel responses to the floods are variable and dependent on the pre-flood ASE, but in general both sandbar size (measured by volume and areal extent) and total sand storage seems to be increasing with HFEs (Hazel et al., 2010; Grams et al., 2013; Mueller et al., 2014). As the grain sizes defined as “sand” (0.063-2mm) are those primarily responsible for building sand bars in Grand Canyon (Rubin et al., 1998; Topping et al, 2005; Schmidt and Grams, 2011a), this paper will focus solely on sand-sized sediment from here on, and the terms “sediment” and “sand” will be used interchangeably unless otherwise stated.

Within Grand Canyon, Marble Canyon is defined as the reach of the Colorado River from Lee’s Ferry to the Little Colorado River confluence approximately 100 km downstream (Fig. 1).

Marble Canyon is considered a critical section of the Colorado River for sandbar restoration, as the Paria River delivers the only significant, reliable sand available within that reach for distribution to sandbars in HFEs (Fig. 3). In the pre-dam era, approximately 22.8 ± 1.2 million metric tons (t) of sand from the upper basin were delivered to Marble Canyon through Glen Canyon, versus only about 1.5 ± 0.3 million t sand from the Paria River (Topping et al., 2000). Now, using estimates from sediment years 2001-2013, Griffiths and Topping (2015) estimate that annual Paria inputs average around 712,000 t sand, and minor tributaries to Marble Canyon supply an average 72,000 t. While the Paria River supplied approximately 6% of the total pre-dam sediment supply to Marble Canyon, the current annual Paria sediment load now supplies over 90% of the total sand available within Marble Canyon for utilization by HFEs; all additional sand is supplied by minor tributaries. As the primary supply of new sediment for Marble Canyon, it is critical that HFEs function as designed and utilize this sand from the Paria River specifically to rebuild sandbars.

This study offers an evaluation of the efficacy with which Paria-derived sand is utilized and retained within Marble Canyon during HFEs. The overarching goal of HFEs is to accumulate sand in Marble Canyon through increased eddy and channel margin storage (U.S. Department of the Interior, 2011). Due to the geometry of the reach, the primary sources of this sand are limited to relict, pre-dam sand and the Paria River; sand from minor tributaries likely represents a much smaller proportion. Within eddy deposition zones, sandbars are assumed to undergo some degree of reworking, evidenced by the increased channel relief moving perpendicular to the flow from sandbar to main channel (Mueller et al., 2014). This reworking process, in addition to executing HFEs such that total Paria-derived sand imports are greater than total exports out of Marble Canyon, suggests an overall accumulation of Paria sand within

Marble Canyon. Sediment mass balances evaluate the magnitude of this accumulation, though compounding uncertainty over multi-year timescales renders necessary an independent assessment of Paria-derived sand retention (Grams et al., 2013). As such, this study investigates the accumulation of Paria-derived sand in Marble Canyon, determining the ratio of Paria-derived to relict, pre-dam sand within HFE deposits throughout the reach.

A geochemically based sediment fingerprint exploiting the different bedrock lithologies from which Upper Colorado River (pre-dam) and Paria River sediments are sourced allows for a quantitative assessment of sediment mixing in sandbars deposited by controlled floods in Marble Canyon. While the Paria River watershed primarily drains Mesozoic terrestrially-sourced sedimentary rocks, many tributaries to the Upper Colorado River have their headwaters in pre-Cambrian igneous and metamorphic rocks (Fig. 4). In some locations, Upper Basin sediments are additionally derived from Tertiary volcanic units. The varying mineralogic assemblages of sediment derived from these different lithologies is reflected in their elemental composition and is measurable by x-ray fluorescence (XRF). In this study, we 1) establish sediment fingerprints based on elemental composition that differentiate the source populations of sand in Marble Canyon, and 2) use those fingerprints in sediment mixing models to determine the relative source contribution to Marble Canyon HFE deposits.

METHODS

Sediment Fingerprinting

This study employs a multi-variate sediment fingerprint based on the bulk elemental composition of the source (relict, pre-dam and Paria River-derived) and mixed (Marble Canyon HFE deposit) sand populations. Elemental composition is one of many physical and chemical characteristics available for use in sediment fingerprints, chosen in this case for its ability to

reflect the mineralogic differences of the source sand populations (Klages and Hseih, 1974, Collins et al., 1996; Collins and Walling, 2002; Gingele and Dekker, 2005; Caitcheon et al., 2006; Collins et al., 2013; Haddadchi et al., 2013, Owens et al., 2016). Additionally, whereas many sediment fingerprinting studies focus on the <63 micron (μm) grain size fraction (Gellis and Walling, 2011; Mukundan et al., 2012; Collins et al., 2013), which often functions as a pollutant in waters with undesirably high turbidity levels, this study focuses on sand sized 63-500 μm. This is also the most prevalent size fraction of sediment in Marble Canyon HFE deposits, therefore the most appropriate for this study (Rubin et al., 1998). To avoid grain size-dependent effects on elemental concentrations (Russel et al, 2001; Koiter et al., 2013;, Smith et al., 2014;, Kraushaar et al., 2015; Smith et al., 2015; Haddadchi et al., 2015; Owens et al., 2016), all sand is separated into six smaller grain size fractions: 63-90, 90-125, 125-180, 180-250, 250-355, and 355-500 μm. Furthermore, this grain size-specific approach allows us to utilize variable mineral compositions unique to each grain size fraction which result from differential weathering rates and styles between minerals. A total of six individual fingerprints based on the bulk elemental compositions of each size fraction from the two source sand populations are the metrics with which six independent mixing models determine the Paria contribution to each size fraction in Marble Canyon HFE deposits.

Sampling Protocol

The sampling protocol in this study was designed to fully characterize the variability in both sand sources for Marble Canyon and the downstream mixed population. Due to the inability to confidently identify and sample pre-dam sand from Marble Canyon downstream of the Paria River confluence, terraces of Upper Basin-derived sediment from pre-dam floods preserved in Lower Glen Canyon are used as a proxy for pre-dam sediment remaining in Marble Canyon. A

total of fourteen samples were taken from three locations in Lower Glen Canyon, all of which were upstream of the first significant gully, Honey Draw. This negates the potential for skewing the composition of pre-dam sand with sediment from the quartz-rich Navajo Sandstone, which forms the canyon walls of Lower Glen Canyon. The sampled terraces are vertically continuous, typically rising 3-5 m above the mean post-dam water level. All samples were taken from below the post-dam high water level to avoid the influence of diagenetic processes (Koiter et al., 2013), as the terraces were often very well consolidated, cemented to a higher degree than the active fluvial sandbars, and had a statistically significant difference in elemental composition from samples taken below the post-dam high water level. The Paria River, draining a 3730 km^2 basin in southern Utah and northern Arizona (Fig. 4), has a relatively low base flow of approximately 5-10 cfs and experiences higher flows primarily due to intense monsoon-driven precipitation in the late summer and early fall (Topping, 1997; Fig. 3a). USGS gauge 09382000 (Fig. 1) records 5-minute data on Paria River discharge and suspended sediment concentration and collects repeated instantaneous suspended sediment samples during such flood events (Fig. 3b). A total of 48 suspended sediment samples from flood events in the 2013 and 2014 monsoon seasons were chosen to represent the Paria River sand population. The composition of sediment delivered during these floods changes as the storm physically moves across the watershed and mobilizes sediment from different lithologic units. To fully account for the variability within Paria-derived sand, a subset of all available suspended sediment samples was chosen based on the rising limbs, peaks, and falling limbs of both discharge and suspended sediment concentration (Fig. 3 a, b; Phillips et al., 2000; Russel et al., 2000) as an alternative to integrated time sampling (Gray and Gartner, 2009; Olley et al., 2016).

A total of 19 Marble Canyon HFE deposits were sampled at fourteen sandbars, twelve of which are long-term monitoring sites where sandbar volume and areal extent is repeatedly measured (Hazel et al., 1999; 2006; 2013); samples of deposits from both the 2013 and 2014 HFEs were collected at six locations (Fig. 5a). At each bar, a trench revealed the internal stratigraphy of the deposit with sedimentary structures that reflect the changing hydrologic and suspended sediment conditions throughout the duration of flood deposition. Typical bar deposits are similar to those reported by Rubin and others (1998) and exhibited some of the signs of suspended sediment supply limitation addressed by Topping and others (2000): coarsening upwards with clay-rich basal layer, main body of (typically) climbing ripples, and uppermost section of planar bedding (Fig. 5b). This stratigraphy was used to ensure that samples were taken solely from the most recent flood deposits following the 2013 and 2014 HFEs. Table 2 contains the year of deposition, location, deposit height, and number of samples per deposit for all HFE deposits used in this study.

Sample Preparation and XRF Testing

Each sample from all three sand populations underwent identical preparation prior to determining their elemental composition. First, samples were sieved into half-phi grain size fractions; the number of samples in each size fraction are summarized in Table 3, and only the size fractions with $n = \geq 10$ were included in further analysis. Following sieving, samples were washed using deionized water and stirred vigorously to break up any clay aggregates and remove coatings on the grains. Dispersion agents were foregone to avoid leaving a chemical trace on the sand grains. Washed samples consisting of one grain size fraction from a single original sample were dried at approximately 250° F (120° C) and transferred to 1.5 x 1.5-inch polyethylene zip-closure bags for testing.

The elemental composition of all samples of the six grain size fractions from each sample of Glen Canyon terraces, Paria River suspended sediment and Marble Canyon HFE deposits were tested using a Niton XLT3-P handheld XRF (Small et al., 2002; Caitcheon et al, 2006; Melquiades et al., 2013; Owens et al., 2016). Each sample was tested three times, measuring 35 major and trace elements during 90-second tests, agitating the sample bag between tests to account for sample heterogeneity. A total of eleven elements were consistently reported for all samples (Table 4): Iron (Fe), Calcium (Ca), Silicon (Si), Phosphorus (P), Sulfur (S), Potassium (K), Chlorine (Cl) , Titanium (Ti), Rubidium (Rb), Strontium (Sr), and Zirconium (Zr). These elemental concentration data serve as the basis for the sediment fingerprint used in the mixing model (Gingele and Deckker et al., 2005; Caitcheon et al., 2006; Hughes et al., 2010). The concentrations of these elements reported by the XRF are not standardized: their proportions relative to each other are consistent but absolute values may be affected by sample thickness, grain orientation, and matrix effects while calculating concentrations from detected x-ray peaks (Sherman, 1955; Castro et al., 2008; Yalcin et al., 2008). Therefore, data were normalized by calculating a total of 55 elemental ratios from the reported concentrations of all combinations of the eleven elements in each individual test. The average value for each ratio across all three tests per grain size sample was then calculated. All six grain size fractions were analyzed independently, determining unique multivariate fingerprints based on these elemental ratios for each fraction, to be used in six independent mixing models. This approach identifies and utilizes the subtle mineralogical differences between each grain size fraction, reflected in elemental compositions measured with XRF, thus creating a more robust analysis than if all size fractions were analyzed in bulk.

Data Preprocessing:

Of the 55 total ratios describing the composition of each sample across all six grain sizes, only a subset passed the standardized test of eligibility for use in the final fingerprints and mixing models (Collins et al., 1996). First, all potential ratios were tested with the Kruskal-Wallis H-test, a non-parametric analysis of variance used to ensure that values between the two and within each of the endmember populations are sufficiently distinct (Collins et al., 1996). Additionally, ratios not eliminated by this requirement must exhibit conservative behavior, maintaining constant values throughout the spatial and temporal timescales of the study (Walling et al., 1993; Small et al., 2002). Given linear additive mixing between two sources, conservativeness also requires that tracer values for the mixed population fall between those of the endmember populations, typically tested with population means (Collins et al., 1996).

A Principal Components Analysis (PCA) consolidated the remaining ratios in each grain size fraction, those eligible for use in the mixing model; the ratios are summarized in Table 5 (Collins et al., 2012; Melquiades et al., 013). PCA effectively combines the eligible ratios into multivariate metrics that best utilize, preserve, and consolidate the variability present in the original ratio data.

Mixing Model

The contribution of Paria-derived sand to Marble Canyon HFE deposits was calculated using a Bayesian mixing model implemented in MixSIAR (Stock and Semmens, 2013), which runs in R (R Core Team, 2016) using JAGS for Markov Chain Monte Carlo (MCMC) simulation (Plummer, 2016). Bayesian models have been gaining traction in sediment fingerprinting studies, partially due to their superior ability to incorporate and propagate uncertainty throughout the

model (Moore and Semmens, 2008; Davis and Fox, 2009; Fox and Papanicolaou, 2009; Parnell et al., 2013; Cooper et al., 2015). MixSIAR is especially valuable for working with a flexible number of tracers as well as continuous or categorical covariates. Though the model was originally developed for dietary analyses in ecological studies, the authors explicitly state its potential for other applications and has previously been used to analyze suspended sediment mixing (Nakayama, 2014).

We ran separate but identical mixing models for each of the six grain sizes, utilizing the unique geochemical signatures for each size fraction. Raw values for the first and second principal components (PC1 and PC2) represented the two sources in MixSIAR. Treating the river mile that describes each site's downstream location as a continuous covariate was considered, though ultimately each site was treated independently due to high variability in the hydraulic nature of eddy-deposition zones and its consequent control on sandbar deposition independent of river mile (Grams et al., 2013). Instead, Marble Canyon data were divided subpopulations by year and site, to calculate the Apparent Paria Percentage (APP) of each HFE deposit individually. A "residual only" error structure was chosen, as the alternative process-based error structures are not appropriate for geologic composition data (Stock and Semmens, 2016b). Given the absence of any definitive prior knowledge on the contribution of Paria-derived sediment to Marble Canyon HFE deposits, an uninformative prior was used. We ran the Markov Chain Monte Carlo (MCMC) procedure in JAGS using three independent "chains", each performing 100,000 MCMC iterations: the first 50,000 iterations were discarded as burn-in, and the sampled results were thinned to 1 in every 50 iterations to remove autocorrelation. Model diagnostics show that this was a sufficient number of iterations, evidenced by the convergence of all chains on the same stationary distribution of parameter values. The reported APP estimate and

uncertainty for each grainsize of all deposits (Figure 7), are the mean and standard deviation values from the resulting posterior distributions.

RESULTS

Principal Components Analysis

The first and second principal components, which jointly explain approximately 60 - 76% of the original variability within the ratio data, were chosen to define each of the sand populations in the fingerprints used by the mixing models (Table 6). We did not use additional PCs as they were unable to distinguish the Glen Canyon and Paria populations, and explained negligible additional variability. Figure 6a depicts how, for each grain size fraction, the values for PC1 and PC2 in all three populations compare. Due to the nature of PCA, the first principal component (PC1) best differentiates the Glen Canyon and Paria sand and thus serves as the primary axis along which all three populations separate (Fig. 6a).

Loadings plots (Fig. 6b) indicate which elemental ratios influence PC1 and PC2, giving insight into how different minerals present in sediment from the two source watersheds influence the fingerprints. Additionally, the ratios with the heaviest loadings on PC1 and PC2 vary for each grain size fraction, thus confirming the utility of analyzing each fraction separately and taking advantage of subtle differences in mineralogic composition between grain size fractions. In the 63-90 fraction, many of the ratios weighing most heavily on PC1 involve Ti, with Ti in the denominator and elements such as K and Si in the numerator on the positive side of the x-axis. This means that as these ratios increase, due to decreasing Ti levels and/or increasing Si and K levels, PC1 values become more positive and characteristic of Paria-derived sand. These ratios and their alignment with PC1 likely reflect differences in the abundance of biotite ($K(Mg, Fe^{2+})_3AlSi_3O_{10}(OH, F)_2$) and amphiboles ($AX_2Z_5((Si, Al, Ti)_8O_{22})(OH, F, Cl, O)_2$) which are

more likely to occur in Glen Canyon sand, versus K-feldspar ($KAlSi_3O_8$) and quartz (SiO_2) which are more abundant in Paria sand. In a similar fashion, ratios in the 90-125 μm fraction such as Fe/S, Rb/Sr, K/Sr, and Ca/Ti suggest that different abundances of iron oxides (Fe_xO_y) and biotite vs. feldspars are likely responsible for the distinction of Glen Canyon and Paria sand along PC1. The 125-180 μm fraction appears to be largely influenced by the presence of zircons (ZrO_2) in the Glen Canyon sand, as shown by the ratios with Zr in the denominator on the Paria side: as Zr levels increase, the value for those ratios decreases thus becoming more like Glen Canyon sand. PC1 in the coarsest three fractions is consistently influenced by ratios with Rb and Sr, and Fe has a strong influence on PC1 in the coarsest two fractions. These ratios likely reflect higher abundances of biotite and iron oxides in the Glen Canyon sand, and more quartz and feldspars in the Paria sand for these fractions.

Mixing Model

The average reported percentage of Paria sand (Apparent Paria Percentage, APP) value for all Marble Canyon deposits from both the 2013 and 2014 HFEs is 44.5%. 2013 HFE deposits have, on average, 33.8 ± 4.1% Paria sand, and range 18.0 – 55.4 %. 2014 HFE deposits have an average 54.7 ± 4.3% APP and range 31.9 – 72.5% APP. These values are derived from the individual, grain-size specific APP measurements at each bar (Fig. 7), using the grain size distribution of each sample and overall proportion of the whole deposit that sample represents to calculate a weighted average. The year-specific estimates of APP are arithmetic averages of the APP values for all sampled deposits in each year.

Absent any prominent trends across all size fractions and deposits, linear or otherwise, grainsize affects APP of individual sandbars to some degree in both 2013 and 2014 (Fig. 7a). In both years, APP in the finest sand fraction (63-90 μm) is consistently lower than the other five

fractions (90-500 μm) at 13 of 19 sampled deposits. Additionally, while the four median size fractions (90-355 μm) show scatter when ordered by river mile, the 355-500 μm fraction shows a slight trend of decreasing APP moving downstream (Fig. 7a).

The average APP for each grain size and, separately for each deposit (using a grain-size distribution weighted average), in each year are shown in Figures 8a and b, respectively. Average APP per grainsize fraction provides an additional perspective on any systematic change in APP with sediment size (Fig. 8a). In both 2013 and 2014, APP is clearly lowest in the finest sand fraction, increasing significantly in the next one (in 2013) or two (in 2014) coarser fractions, followed by a steady decline in APP with further coarsening. When sorted by river mile (Fig. 8b), the data remain scattered and do not show a trend in APP dependent on distance downstream from the Paria River confluence.

Finally, the range in APP for each of the size fractions across all deposits sampled for each year (Fig. 8c.) potentially provides further insight into how different grain sizes of sand behave in this system. Initially, the range in APP appears to increase with coarsening grain size in both years, though a large part of this trend is due to relatively low ranges in the finest fraction. Omitting the finest fraction, there is still a slight increasing trend in the range of reported APP values with increasing grain size fraction, though less so in 2013 than 2014. Looking at the deposit-specific APP values used to calculate these ranges, several sites often have relatively high APP values (those at river mile 22.1 and 30.4) while others tend to have lower APP values (river mile 29.3, 41.4, and 44.5, and 50.2). These patterns do not, however, hold up across all grain sizes at these sites (Fig. 7b).

DISCUSSION

Mixing Model Results

The average APP values in Marble Canyon deposits from the 2013 and 2014 HFEs of 33.8 ± 4.1% and 54.7 ± 4.3%, respectively, are lower than initially expected. HFEs are operated under the assumption that the Paria sediment supplied to the mainstem Colorado River in the months prior to a flood event is the primary supply of sediment available for deposition during HFEs (Department of the Interior, 2011). Based on this assumption, and an assumption by the authors that Marble Canyon HFE deposits comprise sand sourced mainly from the Paria River ASE immediately preceding the flood, APP values for the 2013 and 2014 HFE deposits were expected to approach 90% Paria, reflecting the current sand supply ratio for Marble Canyon. While surprising, the lower observed APP values, and the apparent lack of correlation between distance downstream and, less so, grain size can provide insight into sediment storage and transport within Marble Canyon. The observed APP values suggest that a much higher degree of mixing between the Paria ASE and pre-existing sand takes place in the post-dam Marble Canyon than initially thought. Additionally, though repeat channel bathymetry and sub-areal sandbar measurements provide an analysis of changes in sand storage in Marble Canyon (Hazel et al., 2006, 2010, 2016; Mueller et al., 2014; Kaplinski et al., 2014, 2017), the absolute sand storage volume within Marble Canyon remains unknown and these lower APP values could potentially indicate a larger total sand supply than expected.

The consistently low observed APP values in the 63 – 90 size fraction suggest the potential significance of additional sand sources on Marble Canyon HFE deposit composition. The constraints of the mixing model used to generate these APP values limited the available sources of sediment to relict, pre-dam sand persisting in Marble Canyon, and sand supplied by

the Paria River. As such, these observed APP values suggest that this finest grain size fraction in Marble Canyon HFE deposits comprises roughly 70-95% pre-dam sand. This is highly improbable: very little pre-dam sand of this size likely remains in Marble Canyon, given the winnowing that would occur during the documented export of sand out of Marble Canyon during normal dam operations (Topping et al., 2010; Grams et al., 2013) and the conclusion by Topping and others (2000) that flows over 200-300 m^3/s (7,060-10,600 cfs) result in export from Marble Canyon. The 63-90 μm fraction of sand is thus likely influenced to a large degree by sand delivered by minor tributaries not accounted for in the current mixing model. The extent to which sand in coarser grain size fractions is affected by minor tributary inputs is unknown. A primary implication of this shortfall in the model is that, assuming the direction of inaccuracy in APP remains constant and consistently overestimates the proportion of pre-dam sand in Marble Canyon HFE deposits, the observed APP values presented here can be considered minimum estimates of the contribution of Paria-derived sand supplied in the post-dam era provides to Marble Canyon HFE deposits.

Perhaps just as informative as trends in APP that depend on grain size or river mile is the prominent scatter in the mixing model results. The source of this scatter could be method based, originating from errors arising from a multitude of potential sources. Sampling the deposits in one location, as opposed to several in different locations throughout the sandbar could affect how representative those samples are of the entire deposit. Characterizing the source sand populations is another plausible source of error. The terraces in Lower Glen Canyon do not necessarily represent the entire sediment population originating in the upper Colorado River Basin and previously supplied to Marble Canyon, but they are the best proxy currently available. A study incorporating historic flows and sediment characterization of individual watersheds within the

Upper Colorado Basin could potentially yield a more accurate characterization. Additionally, only the Paria sediment supplied prior to the 2013 and 2014 HFEs was used to characterize the Paria River sediment population, as they seemed most appropriate for studying deposits from the 2013 and 2014 HFEs. Additional samples from previous and following years may be necessary to fully characterize the variability within Paria River sediment composition. While testing with XRF, three individual tests accounted for heterogeneity within the sample contained within the testing bag, though the degree to which this small sample represents that grain size throughout an entire deposit is unknown and could be a further source of error. In the XRF data, the use of elemental ratios reduced but potentially did not fully negate the error introduced by matrix effects in the conversion of x-ray intensity curves to elemental concentrations (Sherman, 1955).

In contrast, the scatter among the mixing model APP results might accurately reflect inherent spatial heterogeneity within the sediment stored in Marble Canyon. The distribution of pools between rapids capable of storing large volumes of sand prior to and from which large volumes of sand are also excavated during HFEs is not spatially consistent throughout Marble Canyon. Certain eddy deposition zones where HFE deposit sandbars form have much larger sand supplies immediately upstream than others (Kaplinski et al., 2014, 2017). This likely affects, on a pool-eddy scale, the degree to which Paria-derived sand accumulates but also the relative influence a given addition of Paria-derived sand would have on the overall composition of sand available for deposition during HFEs. Evidence for significant recycling between eddy sandbar deposits and the immediately adjacent channel (Mueller et al., 2014) incites questions of sediment residence time and the degree to which new sediment is incorporated into these deposits compared to storage in the main channel. A high degree of spatial heterogeneity also exists within overall sandbar response to HFEs, as local hydraulic effects and channel geometry

control the morphodynamic response of sandbars during HFEs more than pre-flood sediment supply (Grams et al., 2013).

Despite the high degree of scatter within the mixing model results, the 2014 APP values are generally higher than those for 2013 HFE deposits (Fig. 8a, b), a discrepancy which potentially yields information about sediment storage and transport during HFEs. It is possible that with each additional HFE, the overall concentration of Paria-derived sand within Marble Canyon increases. APP levels could also be sensitive to additional variables unique to each flood event. The 2013 and 2014 HFEs had identical durations but the maximum released discharges were 34,100 cfs (965 m^3/s) and 38,400 cfs (1090 m^3/s), respectively; the larger release yielded higher APP values. The timing of Paria sediment delivery to the main stem Colorado River and the magnitude of water releases from Glen Canyon dam prior to a flood may influence characteristics of the ASE such as grain size distribution, due to the winnowing of fines during normal dam operations prior to a flood, that affect the resulting Paria contribution to flood deposits. Figure 9 shows the cumulative sediment load delivered to the main stem Colorado by the Paria River in both 2013 and 2014 (Fig. 9a and b, respectively) and the corresponding flows on the Colorado River (Fig. 9c, d). In 2013, two smaller flood events preceded one large sediment delivery on September 8-14 (Fig. 9a). Following this large flood event, the Colorado River experience three distinct flow regimes in September, October, and November (Fig. 9c) prior to the 2013 HFE. In 2014, Paria sediment was supplied to the main stem in four more evenly-sized deliveries, three of which took place in September (Fig. 9b), and was subjected to two distinct flow regimes prior to the flood (Fig. 9d).

In a larger perspective, the overall volume of available Paria-derived sand may have the most influence on the composition of HFE deposits. The total Paria ASE volume was 1,918,000 tons in 2013, compared to 1,280,000 in 2014, a 33% reduction (www.gcmrc.gov/discharge_qw_sediment). Following the 2013 HFE, roughly 1,000,000 t sand remained in upper Marble Canyon (approximately river miles 0 – 30) prior to the 2014 Paria sand delivery. Lower Marble Canyon (river miles 30 – 62, appx.) experienced a net gain of approximately 270,000 t sand during the 2013 flood and continued accumulating more than 300,000 t sand prior to the 2014 flood (www.gcmrc.gov/discharge_qw_sediment). Thus the total volume of available sand prior to the flood was greater in 2014 than in 2013.

Topping and others (2007) concluded that the grain size distribution of Paria ASE can significantly influence the suspended sediment concentration and consequently deposition in eddy sandbars during floods. The degree to which this affected the observed Paria contribution levels in the 2013 and 2014 Marble Canyon HFE deposits is unclear, as the grain size distributions of sand delivered by the Paria River prior to the two floods are nearly identical. Interestingly, the modal grain size fraction in both years of Paria-derived sand at the time it was delivered to the main stem Colorado River was the 90 – 125 μm fraction, compared to the 125 – 180 μm fraction in HFE deposits from both years. Without additional years of APP data, it is not possible to thoroughly evaluate how each of these variables influences the Paria contribution to HFE deposits or how those APP levels will change without time, though such information would likely help optimize HFE flood design and maximize the retention of Paria derived sediment in Marble Canyon.

Modeling Paria Sand Integration into Marble Canyon Storage

Though initially lower than expected the observed APP levels from the 2013 and 2014 HFE deposits are more reasonable when considering the sediment dynamic of storage and transport that take place both during HFEs and in the preceding sediment enrichment period. The incoming Paria sediment, when delivered, is subject to transport in the flows released during normal dam operations. The finer silt and clay grainsizes often stay in suspension, and the remaining sand is gradually winnowed out of the bed, getting progressively coarser, with normal dam releases (Topping et al., 2010). This veneer of Paria-supplied sand is mobilized first during floods, and at least partly exported from Marble Canyon; the amount and grain size distribution of the wave of mobilized antecedent sand enrichment is measurable with acoustic-Doppler profilers located downstream of Marble Canyon (Topping et al., 2010). Because this sand is so readily mobilized during floods, it is unreasonable to assume that 100% of the antecedent sand enrichment will be retained in Marble Canyon channel storage and is instead exported. Most likely, some portion of the "new" sand is incorporated into the active mixing layer of sediment, which experiences scour and fill during normal dam operations and floods, while the remaining sand is flushed downstream. Thus, Paria sand is slowly incorporated into the active layer, gradually replacing and supplementing the relict, pre-dam sand still in the channel.

In the five decades since Glen Canyon Dam was completed, the average Paria contribution to Marble Canyon sandbars has increased from, presumably, 6% to an average of 44%. By assuming the composition of the sand in HFE deposits accurately represents the composition of the active storage within the Marble Canyon channel, we can calculate the proportion of each annual Paria influx that needs to be incorporated into the Marble Canyon active storage to achieve the observed APP levels. This allows us to determine how effective

HFEs are in capturing Paria sediment to use in sandbar restoration. The presented model (Fig. 10) calculates the continuous increase in Paria contribution to Marble Canyon storage using the equation:

$$Fp_{t+1} = \frac{(Fp_t)(Mm_t) - (Fp_t)((Mm_t)(Rr) - \Delta S) + (Mp_{in})(Rr)}{Mm_t + \Delta S} \quad (1)$$

where Fp_t is the fraction of Paria-derived sand in the total Marble Canyon storage in year t after the dam's completion; Fp_{t+1} is the fraction of Paria-derived sand in the total Marble Canyon storage the following year. The expression:

$$(Fp_t)(Mm_t) \quad (2)$$

describes the mass of Paria-derived sand in Marble Canyon in year t; Mm_t is the mass of sand stored in Marble Canyon in year t. The expression:

$$(Fp_t)((Mm_t)(Rr) - \Delta S) \quad (3)$$

describes the mass of Paria-derived sand exported from Marble Canyon between year t and $t+1$. Mp_{in} is the mass of Paria sand delivered to the main stem Colorado year t, and Rr is the proportion of that sand retained within Marble Canyon, integrated into the active sediment storage. ΔS is the change in total Marble Canyon storage from year t to year $t+1$. The expression:

$$(Mp_{in})(Rr) \quad (4)$$

describes the mass of Paria sand retained in Marble Canyon from year t to year $t+1$. The expression in the denominator describes the total storage in Marble Canyon in year $t+1$:

$$Mm_t + \Delta S \quad (5)$$

The initial fraction of Paria-derived sand within Marble Canyon when the dam closed in 1963, at time at $t=0$, is assumed to match the pre-dam supply ratio of Upper Colorado River Basin to Paria River sand of 6% (Griffiths and Topping, 2015; Topping et al., 2000). Though a significant volume of sand was likely evacuated from Marble Canyon following the dam's completion, we first run a simplified model assuming constant storage of 26.2 million tons (t), based on the estimates by Hazel and others (2006): total active storage within eddy deposition zones was determined to be 13.1 million t and assumed to comprise half the total active storage in Marble Canyon, including channel storage. Additionally, three scenarios test the sensitivity of the required Paria sand retention rate necessary to achieve current observed APP levels to changing total Marble Canyon storage. We consider a 10%, 30%, and 50% reduction in Marble Canyon storage starting in 1963 to reach 26.2 million t in 1996, when high flow experiments began. These scenarios reflect the sediment evacuation that likely occurred from Marble Canyon during a series of 14 pulsed high flows in 1965 that caused intense scouring of Lower Glen Canyon (Grams et al., 2007).

In all four conditions tested, the required retention rate of the annual Paria sand load in Marble Canyon to reach an average APP of 44% by the year 2014 ranged from 20.2 – 29.7% (Fig. 11). When Marble Canyon storage (*Mm*) was assumed to remain constant from 1963 – 2014, the fraction of Paria sand within Marble Canyon (*Fp*) increased at a constant rate (Fig. 11). If Marble Canyon storage is assumed to have decreased by 10%, 30%, or 50%, *Fp* increases at an increasing rate, until 1996 when it increases at a slower linear rate than with constant storage. This effect is exaggerated as the amount by which *Mm* decreased from 1963-2014 increases from 10% to 50%. In all scenarios, *Fp* is approximately the same in the early 1990s, then *Fp* in the

changing-storage scenarios diverges until 1996, and converges again to the average observed APP of approximately 44% in 2014.

While it is unlikely that the retention rate of Paria-derived sand in the active Marble Canyon storage has remained constant throughout each year since 1963, this retention rate model provides a rough estimation. Higher percentages of Paria sand are likely integrated into Marble Canyon storage during HFEs, though it is difficult to say how much higher retention rates would be than predicted in this model. It seems plausible, however, that during HFEs, which are designed specifically to incorporate Paria sand into Marble Canyon storage, Paria sand retention rates would exceed the relatively low rates of 20-30% required in all seven tested scenarios.

Sediment transport occurs throughout the entire year in Marble Canyon, supporting the idea that integration of Paria sand also occurs on a daily basis. Continuously monitored sediment transport data within and leaving Marble Canyon (www.gcmrc.gov/discharge_qw_sediment) reveal temporal patterns of sediment enrichment and depletion in Marble Canyon. During sediment enrichment periods, upper Marble Canyon (river miles 30-60) storage increases, sometimes substantially, with sufficient Paria flux. Simultaneous, export out of upper Marble Canyon can increase storage into lower Marble Canyon (river miles 30-60). During floods, upper Marble Canyon experiences a negative sand mass balance characterized by sand export, and LMC tends to have either a neutral or slightly negative sand mass balance (with exports roughly equaling or slightly exceeding imports from upper Marble Canyon) (Mueller et al., 2014). This pattern of mass transport suggests that a majority of mixing within the channel active layer likely occurs during HFEs specifically. Transport between Upper and Lower Marble Canyon suggests that there is some degree, though minor, of mixing during interim flows between floods. Upwellings of water in the main channel that contain low concentrations of suspended sediment

can be observed both while on the water or at higher elevation vantage points during interim flows. The plumes are visible when the water is "green", and relatively clear of the silt and mud responsible for turning the water red-brown and thick with mud during monsoon season, which further supports that the sediment being mixed is indeed sand. Because finer sand will be more easily entrained in these plumes, it is possible that the finer sand fractions of Paria influxes are more readily incorporated into the active sediment layer than coarser sizes. This would help explain the trends in APP with grainsize shown in Figure 8. Fractionation effects such as this also likely occur during floods themselves, and help explain the decrease in APP with river mile in the 355-500 μm grain size fraction. Because the coarser grains are not entrained as readily as finer grains, the "wave" of increased APP due to mixing could likely travel downstream more slowly in this coarsest grain size.

CONCLUSIONS

This study presents a relatively novel application of sediment fingerprinting techniques, evaluating the sustainability of fluvial restoration efforts focused on promoting downstream aggradation, as opposed to preventing upstream erosion. In line with the continuing goals of the Grand Canyon Adaptive Management Program, this study helped expand our knowledge of sediment dynamics in the post-dam Colorado River in Grand Canyon. A multivariate fingerprint for Glen Canyon (acting as a proxy for relict, pre-dam sand in Marble Canyon) and Paria River sand was derived from elemental data that reflected the differences in mineralogy of their respective watershed lithologies. Following the methods of other sediment fingerprinting studies, these elemental data were measured using XRF (Gingele and Deckker, 2005; Caitcheon et al., 2006; Hughes et al., 2010; and Melquiades et al., 2013), underwent standard statistical procedures (Collins et al., 1996, Walling et al., 1999) to determine which data were eligible for

use in a mixing model, and combined into a multivariate composite fingerprint using a principal components analysis (Melquiades et al., 2013; Collins et al., 2012). This multivariate signal was used in a Bayesian mixing model, MixSIAR (Semmens and Stock, 2016) to determine the apparent contribution of Paria-derived sand in Marble Canyon HFE deposits.

In order for the current GCMRC sandbar management practices to be sustainable, the long-term erosional trend that exists in the post-dam Colorado River through the Marble Canyon reach of Grand Canyon needs to be reversed (Schmidt and Grams, 2011b). In a sense, the only way to do this is to increase the mass of sand stored in Marble Canyon through the incorporation of tributary-supplied sediment. The extent to which this incorporation has occurred in the last 20 years of controlled floods can be evaluated with the fraction of Paria-derived sand in Marble Canyon HFE deposits calculated in this study. The results are variable among both different grain size fractions and sandbar locations, though this is not surprising given the spatial heterogeneity of channel sand storage and local hydraulic effects on sand deposition (Grams et al., 2013; Kaplinski et al., 2014, 2017). Despite the inconsistent APP values, only two out of 112 samples (each representing one grain size fraction from one deposit), were below the initial assumed APP of 6%, and the upper uncertainty bound for both samples exceeded 6%. In light of this, and that the average APP for each year that far exceeds 6%, it is clear that sand delivered to Marble Canyon is actively being incorporated into the active sediment layer.

Any number of variables can affect the percentage of Paria sand within an individual deposit. Characteristics of the Paria sediment enrichment including the total sand mass delivered to the Colorado River, when those delivery events occur, and the grain size distribution of the delivered sediment all likely affect the APP of deposits created during an HFE. Characteristics of HFEs such as flood magnitude and duration may systematically control APP, and spatial

heterogeneity in the Marble Canyon channel upstream or adjacent to eddy deposition zones and local hydraulic effects may ultimately cause scatter in APP to persist. More years of data are necessary to confirm trends in APP either through time, by grain size, or by river mile, but also to establish any correlations between APP and any number of potentially influential factors. Further studies should aim to 1) better characterize the source populations with more robust sampling approaches and/or larger data sets, and 2) include minor tributaries as a third sediment source, to establish the minor tributary contribution to not only the finest sand fractions within HFE deposits, but the coarser fractions as well.

Calculated, constant, retention rates of Paria-derived sand required to reach the observed APP levels are reasonable, thus suggesting that Paria sand has been, and will continue to be, integrated into Marble Canyon. The rates describing scenarios of constant integration are low enough such that the expected, elevated integration rates of Paria sand during HFEs should be attainable. Once the Paria-derived sand is incorporated into the active sediment in Marble Canyon, HFEs are largely responsible for creating and maintaining the deposits in which sand is stored, postponing and mitigating downstream transport out of Marble Canyon. Thus, provided Marble Canyon exports during flood events do not exceed the antecedent sand enrichment that persists prior to floods, and that floods are conducted at frequent enough intervals to maintain the deposit in which sand is stored (Grams et al., 2013), HFEs can be considered conditionally sustainable.

REFERENCES

Barthod, L.R.M., Liu, K., Lobb, D.A., Owens, P.N., Martinez-Carreras, N., Koiter, A.J., Petticrew, E.L.,McCullough, G.K., Liu, C., Gaspar, L., 2015, Selecting color-based tracers and classifying sediment sources in the assessment of sediment dynamics using sediment source fingerprinting. Journal of Environmental Quality, v. 44, pp. 1605–1616.

Brown, A. G., Carey, C., Erkens, Gilles, Fuchsm M., Hoffman, T., Macaire, J., Moldenhauer, K., Walling, D. E., 2009, From sedimentary records to sediment budgets: Multiple approaches to catchment sediment flux: Geomorphology, v. 108, pp. 35-47.

Caitcheon, G., Douglas, G., Palmer, M., 2006, Sediment Source Tracing in the Lake Burragorang Catchment: SCIRO Land and Water Science Report 47/07, 29 p

Castro, K., Pessanha, S., Proietti, N., Princi, E., Capitani, D., Carvalho, M.L., Madariaga, J.M., 2008, Noninvasive and nondestructive NMR, Raman and XRF analysis of a Blaeu coloured map from the seventeenth century: Anals of Bioanalytical Chemistry, v. 391, pp. 433–441.

Collins AL, Walling DE, Leeks GJL, 1996a, Composite fingerprinting of the spatial source of fluvial suspended sediment: a case study of the Exe and Severn river basins, United Kingdom: Geomorphologie: Relief, Process, Environment, v. 2, pp. 41-53.

Collins AL, Walling DE, Leeks GJL, 1996b, Use of composite fingerprints to determine the provenance of the contemporary suspended sediment load transported by rivers: Earth Surface Processes and Landforms, v. 32, pp. 31-52.

Collins AL, Zhang Y, Duethmann D, Walling DE, Black KE, 2013, Using a novel tracing-racking framework to source fine-grained sediment loss to watercourses at catchment scale. Hydrological Processes, v. 27, pp. 959–974

Collins AL, Zhang Y, Walling DE, Grenfell SE, Smith P, 2010, Tracing sediment loss from eroding farm tracks using a geochemical fingerprinting procedure combining local and genetic algorithm optimization: Science of the Total Environment, v. 408, pp. 5461–5471.

Collins, A. L., Naden, P. S., Sear, D. A., Jones, J. I., Foster, I. D., Morrow, K., 2011, Sediment targets for informing river catchment management: international experience and prospects: Hydrological Processes, v. 25, pp. 2112-2129.

Collins, A. L., Walling, D. E., 2002, Selecting fingerprint properties for discriminating potential suspended sediment sources in river basins: Journal of Hydrology, v. 261, pp. 218-244.

Collins, A.L., Zhang, Y., McChesney, D., Walling, D.E., Haley, S.M., Smith, P., 2012, Sediment source tracing in a lowland agricultural catchment in southern England using a modified procedure combining statistical analysis and numerical modelling. Science of the Total Environment, v. 414, pp. 301–317.

Cooper, R.J., Krueger, T., Hiscock, K.M., Rawlins, B.G., 2015, High temporal resolution fluvial sediment source fingerprinting with uncertainty: a Bayesian approach: Earth Surface Processes and Landforms, v. 40, pp. 78–92.

Davis, C. M., Fox, J. F., 2009, Sediment Fingerprinting: Review of the Method and Future improvements for allocating nonpoint source pollution: Journal of Environmental Engineering, v. 135, no. 7., pp. 490-504.

Department of the Interior, 2011, Environmental Assessment – Development and Implementation of a Protocol for High-Flow Experimental Releases from Glen Canyon Dam, Arizona, 2011 through 2020: Washington, D.C., Office of the Secretary of the Interior, Bureau of Reclamation, 546 p.

Fox, J. F., Papanicolaou, A., N., 2008, An un-mixing model to study watershed erosion processes: Advances in Water Resources, v. 31, pp. 96-108.

Gellis AC, Hupp CR, Pavich MJ, Landwehr JM, Banks WSL, Hubbard BE, Langland J, Ritchie JC, Reuter JM, 2009, Sources, transport, and storage of sediment at selected sites in the Chesapeake Bay Watershed: US Geological Survey Scientific Investigations Report 2008–5186, 110 p.

Gellis, A., Walling, D. E., 2011, Sediment Source Fingerprint (Tracing) and Sediment Budgets as Tools in Targeting River and Watershed Restoration Programs: Geophysical Monograph Series 194, pp. 263-291

Gingele, F. X. and Deckker, P. DE., 2005, Clay mineral, geochemical, and Sr-Nd isotopic fingerprinting of sediments in the Murray-Darling fluvial system, southeast Australia: Australian Journal of Earth Sciences, 2005, v. 52, pp. 965-974.

Graf, W. L., 2006, Downstream hydrologic and geomorphic effects of large dams on American rivers: Geomorphology, 79, pp. 336-360.

Grams, P. E., Topping, D. J., Schmidt, J. C., Hazel et al., J. E., Kaplinski, M., 2013, Linking Morphodynamic response with sediment mass balance on the Colorado River in Marble Canyon: Issues of scale, geomorphic setting, and sampling design: Journal of Geophysical Research: Earth Surface, v. 118, pp. 361-381.

Grams, P., Schmidt, J., Topping, D., 2007, The rate and pattern of bed incision and bank adjustment on the Colorado River in Glen Canyon downstream from Glen Canyon Dam, 1956-2000: GSA Bulletin, v. 119, no. 5/6, pp. 556-575.

Gray, J. R., and Gartner, J. W., 2007, Technological advances in suspended-sediment surrogate monitoring: Water Resources Research, v. 45, W00D29, doi:10.1029/2008WR007063.

Griffiths, R., E., Topping, D. J., 2015, Inaccuracies in sediment budgets arising from estimations of tributary sediment inputs: an example from a monitoring network on the Southern Colorado Plateau, in Technical Papers, 3rd Joint Federal Sedimentation and Hydrology Interagency Conference, Reno, NV, April 19-23, 12p.

Haddachi, A., Olley, J., Pietsch, T., 2015, Quantifying sources of suspended sediment in three size fractions: Journal of Soils Sediments, v. 15, pp. 2086–2100.

Haddadchi, A., Ryder, D.S., Evrard, O., Olley, J., 2013, Sediment fingerprinting in fluvial systems: review of tracers, sediment sources and mixing models: International Journal of Sediment Research, v. 28, pp. 560–578.

Hardy, F., Bariteau, L., Lorrain, S., Theriault, L., Gagnon, G., Messier, D., Rougerie, J-F., 2010, Geochemical tracing and spatial evolution of the sediment bed load of the Romaine River, Quebec, Canada: Catena, v. 81, pp. 66-76.

Hazel, J.E., Jr., Grams, P.E., Schmidt, J.C., and Kaplinski, Matt, 2010, Sandbar response in Marble and Grand Canyons, Arizona, following the 2008 high-flow experiment on the Colorado River: U.S. Geological Survey Scientific Investigations Report 2010–5015, 52 p.

Hazel, J.E., Jr., Topping, D.J., Schmidt, J.C., and Kaplinski, Matt, 2006, Influence of a dam on fine-sediment storage in a canyon river: Journal of Geophysical Research, v. 111, no. F01025, p. 1–16, doi:10.1029/2004JF000193.

Hughes, A.O., Croke, J.C., Pietsch, T.J., Olley, J.M., 2010, Changes in the rates of floodplain and in-channel bench accretion in response to catchment disturbance, central Queensland, Australia: Geomorphology, v. 114, 338–347.

Kaplinski, M., Hazel, J.E., Jr., Grams, P.E., Davis, P.A., 2014, Monitoring fine-sediment volume in the Colorado River ecosystem, Arizona—Construction and analysis of digital elevation models: U.S. Geological Survey Open-File Report 2014–1052, 29 p., doi: 10.3133/ofr20141052.

Kaplinski, M., Hazel, J.E., Jr., Grams, P.E., Kohl, Keith, Buscombe, D.D., and Tusso, R.B., 2017, Channel mapping river miles 29–62 of the Colorado River in Grand Canyon National Park, Arizona, May 2009: U.S. Geological Survey Open-File Report 2017–1030, 35 p., https://doi.org/10.3133/ofr20171030.

Kearsely, L. H., Schmidt, J. C., Warren, K. D., 1994, Effects of Glen Canyon Dam on Colorado River sandbar deposits used as campsites in Grand Canyon National Park, USA: River and Research Applications, v. 9, iss. 3, pp. 137-149.

Klages, M. G., Hsieh, Y. P., 1975, Suspended solids carried by the Galatin River of Southwestern Montana: II. Using mineralogy for inferring sources. Journal of Environmental Quality, v. 4, pp. 68-73.

Koiter, A.J., Owens, P.N., Petticrew, E.L., Lobb, D.A., 2013, The behavioural characteristics of sediment properties and their implications for sediment fingerprinting as an approach for identifying sediment sources in river basins: Earth Science Review, v. 125, pp. 24–42.

Kraushaar, S., Schumann, T., Ollesch, G., Schubert, M., Vogel, H.J., Siebert, C., 2015, Sediment fingerprinting in northern Jordan: element-specific correction factors in a carbonatic setting: Journal of Soils Sediments, v. 15, pp. 2155–2173.

Laceby, J. P., McMahon, J., Evrard, O., Olley, J., 2015, A comparison of geological and statistical approaches to element selection for sediment fingerprinting: Journal of Soils and Sediments, v. 15, pp. 2117-2131, doi: 1 0.1007/s11368-015-1111-9.

Lane, E.W., 1955, The importance of fluvial morphology in hydraulic engineering: Proceedings of the American Society of Civil Engineers, v. 81, paper 745, pp. 1–17.

Lehner, B., Verdin, K., Jarvis, A., 2006, HydroSHEDS Technical Documentation. World Wildlife Fund US, Washington, DC. Available at http://hydrosheds.cr.usgs.gov.

Leopold, L.B., Maddock, Thomas, Jr., 1953, The hydraulic geometry of stream channels and some physiographic implications: U.S. Geological Survey Professional Paper no. 252, 53 p.

Ludington, S., Moring, b.S., Miller, R.J., Stone, P.A., Bookstrom, A.A., Bedfor, D.R., Evans, J.G., Haxel, G.A., Nutt, C.J., Flyn, K.S., Hopkins, M.J., 2007, Preliminary integrated geologic map databases for the United States: Western States: U.S. Geological Survey Open-File Report 2005-1305, scale 1:500,000.

Magilligan, F. J., Nislow, K. H., 2005, Changes in hydrologic regime by dams: Geomorphology, 71, pp. 61-78.

Maher, B. A., Watkins, S. J., Brunskill, G., Alexander, J., Fieldings, C. R., 2008, Sediment provenance in a tropical fluvial and marine context by magnetic ‘fingerprinting’ of transportable sand fractions: Sedimentology, 21 p.

Melis, T. S., ed., 2011, Effects of three high-flow experiments on the Colorado River ecosystem downstream from Glen Canyon Dam, Arizona: U.S. Geological Survey Circular 1366, 147 p.

Melquiades FL, Andreoni LFS, Thomaz EL, 2013, Discrimination of landuse types in a catchment by energy dispersive X-ray fluorescence and principal component analysis: Applied Radioactive Isotopes, v. 77, pp. 27–31

Minella, J. P. G., D. E. Walling, and G. H. Merten, 2008, Combining sediment source tracing techniques with traditional monitoring to assess the impact of improved land management on catchment sediment yields: Journal of Hydrology, v. 348, no. (3–4), pp. 546–563.

Minella, J. PG., Merten, G. H., Walling, D. E., Reichert, J. M., 2009, Changing sediment yield as an indicator of improved soil management practices in southern Brazil: Catena, v. 79, pp. 228-236.

Moore, J. W., & Semmens, B. X, 2008, Incorporating uncertainty and prior information into stable isotope mixing models. Ecology Letters, v. 11, no. 5, pp. 470-480.

Mueller, E. R., Grams, P. E., Schmidt, J. C., Hazel, J. E., Alexander, J. S., Kaplinski, M., 2014, The influence of controlled floods on fine sediment storage in debris fan-affected canyon of the Colorado River basin: Geomorphology, 226, p. 65-75.

Mukundan, R., Walling, D.E., Gellis, A.C., Slattery, M.C., Radcliffe, D.E., 2012, Sediment source fingerprinting: transforming from a research tool to a management tool: Journal of the American Water Resource Association, doi:10.1111/j.1752-1688.2012.00685

Nakayama, K., Beitia, C., Ohtso, N., Yamasaki, S., Yasayuki, M., Yamane, M., 2014, Fingerprint methods for suspended sediment transport processes by using X-ray fluorescence analysis: Abstract H51O-0811 presented at the 2014 Fall Meeting, AGU, San Francisco, California, 15-19 December.

Olley JM, Burton J, Smolders K, Pantus F, Pietsch T, 2013, The application of fallout radionuclides to determine the dominant erosion process in water supply catchments of subtropical South-east Queensland, Australia: Hydrologic Processes, v. 27, pp. 885–895.

Owens, P. N., Blake, W. H., Gaspar, L., Gateuille, D., Koiter, A. J., Lobb, D. A., Petticrew, E. L., Reiffarth, D. G., Smith, H. G., Woddward, J. C., 2016, Fingerprinting and tracing the sources of soils and sediments: Earth and ocean science, geoarchaeological, forensic, and human health applications: Earth-Science Reviews, v. 162, pp. 1-23.

Parnell, A. C., Inger, R., Bearhop, S., & Jackson, A. L., 2010, Source partitioning using stable isotopes: coping with too much variation. PLoS One, v.5, no.3, e9672.

Parnell, A. C., Phillips, D. L., Bearhop, S., Semmens, B. X., Ward, E. J., Moore, J. W., Jackson, A. L., Grey, J., Kelly, D. J., and Inger, R, 2013, Bayesian stable isotope mixing models: Environmetrics, v. 24, no. 6, pp. 387-399.

Petts, G. E., Gurnell, A. M., 2005, Dams and geomorphology: Research progress and future directions: Geomorphology, no. 71, p. 27-47.

Phillips, J.M., M.A. Russell, and D.E. Walling, 2000, Time-Integrated Sampling of Fluvial Suspended Sediment: A Simple Methodology for Small Catchments: Hydrological Processes v. 14, pp. 2589-2602.

Plummer, M., 2016, rjags: Bayesian Graphical Models using MCMC. R package version 4-6. https://CRAN.R-project.org/package=rjags.

Poff, N. L., Allan, J. D., Bain, M. B., Karr, J. R., Prestegaard, K. L., Richter, B. D., Sparks, R. E., Stromberg, J. C., 1997, The Natural Flow Regime: BioScience, v. 47, no. 11, pp. 769-784.

R Core Team, 2016, A language and environment for statistical computing: R Foundation for Statistical Computing, Vienna, Austria. URL https://www.R-project.org/.

Rotman, R., Naylor, L., McDonnel, R., MacNiocaill, C., 2008, Sediment transport on the Freiston Shore managed realignment site: An investigation using environmental magnetism: Geomorphology, v. 100, pp. 241-255.

Rubin, D.M., Nelson, J.M., and Topping, D.J., 1998, Relation of inversely graded deposits to suspended-sediment grain-size evolution during the 1996 flood experiment in Grand Canyon: Geology, v. 26, no. 2, pp. 99–102.

Russell, M.A, D.E. Walling, and R.A. Hodgkinson, 2000, Appraisal of a Simple Sampling Device for Collecting Time-Integrated Fluvial Suspended Sediment Samples. In: The Role of Erosion and Sediment Transport in Nutrient and Contaminant Transfer. IAHS Publication No.263, M. Stone (Editor). IAHS Press, Wallingford, United Kingdom, pp. 119-127.

Schmidt, J. C., 1999, Summary and synthesis of geomorphic studies conducted during the 1996 controlled flood in Grand Canyon, *in* Webb, R. H., Schmidt, J. C., Marzolf, G. R., Valdez, R. A., eds. The Controlled Flood in Grand Canyon, American Geophysical Union Geophysical Monograph 110, Washington, D. C., USA, pp. 329-341.

Schmidt, J. C., and D. M. Rubin, 1995, Regulated streamflow, fine-grained deposits, and effective discharge in canyons with abundant debris fans, in Natural and Anthropogenic Influences in Fluvial Geomorphology: The Wolman Volume, Geophysical Monograph Series, v. 89, edited by J. E. Costa et al., pp. 177– 195, AGU, Washington, D. C.

Schmidt, J.C., and Grams, P.E., 2011a, The high flows—Physical science results, *in* Melis, T.S., ed., Effects of three high-flow experiments on the Colorado River ecosystem downstream from Glen Canyon Dam, Arizona: U.S. Geological Survey Circular 1366, pp. 53–91.

Schmidt, J.C., and Grams, P.E., 2011b, Understanding Physical Processes of the Colorado River, *in* Melis, T.S., ed., Effects of three high-flow experiments on the Colorado River ecosystem downstream from Glen Canyon Dam, Arizona: U.S. Geological Survey Circular 1366, pp. 53–91.

Schmidt, J.C., and Wilcock, P.R., 2008, Metrics for assessing the downstream effects of dams: Water Resources Research, v. 44, no. W04404, p. 1–19, doi:10.1029/2006WR005092

Schmit, L., Gloss, S., Updike, C., 2005, Overview, *in* Gloss, S., Lovich, J. E., Melis, T. S., 2005, The state of the Colorado River Ecosystem in Grand Canyon: A report of the Grand Canyon Monitoring and Research Center 1991-2004: USGS Circular 1282, pp. 1-16.

Sherman, J., 1955, The theoretical derivation of fluorescent X-ray intensities from mixtures: Spectrochimica Acta, v. 7, pp. 283-306.

Slattery, M.C., J. Walden, and T.P. Burt, 2000, Fingerprinting Suspended Sediment Sources Using Mineral Magnetic Measurements: A Quantitative Approach, In: Tracers in Geomorphology, I. Foster (Editor). John Wiley & Sons, Chichester, pp. 309-322.

Slattery, M.C., T.P. Burt, and J. Walden, 1995, The Application of Mineral Magnetic Measurements to Quantify Within-Storm Variations in Suspended Sediment Source. International Association of Hydrological Sciences Publication no. 229, pp. 143-151.

Small, I.F., J.S. Rowan, S.W. Franks, A. Wyatt, and R.W. Duck, 2004, Sediment Fingerprinting Using a Bayesian Approach Yields a Robust Tool for Environmental Forensic Applications, *in*: Environmental Forensics, D.A. Croft and K. Pye (Editors). Geological Society Special Publication, London, pp. 235-248.

Smith, H.G., Blake, W.H., 2014, Sediment fingerprinting in agricultural catchments: a critical re-evaluation of source discrimination and data corrections: Geomorphology, v. 204, pp. 177–191.

Stock, B. C. and B. X. Semmens, 2013, MixSIAR GUI User Manual. Version 3.1. https://github.com/brianstock/MixSIAR/. doi:10.5281/zenodo.47719.

Stoeser, D.B., Green, G.N., Morath, L.C., Heran, W.D., Wilson, A.B., Moore, D.W., Van Gosen, B.S., 2007, Preliminary integrated geologic map databases for the United States: Central States: U.S. Geological Survey Open-File Report 2005-1351, scale 1:500,000.

Syvitski, J.P.M., Vorosmarty, C.J., Kettner, A.J., Green, P., 2005, Impact of humans on the flux of terrestrial sediment to the global coastal oceans: Science, v. 308, pp. 376-370.

Topping, D. J., 1997, Physics of flow, sediment, transport, hydraulic geometry, and channel geomorphic adjustment during flash floods in an ephemeral river, the Paria River, Utah and Arizona [Ph. D. thesis]: University of Washington, 377 p.

Topping, D. J., Rubin, D., Vierra, L., 2000, Colorado River sediment transport: pt. 1: natural sediment supply limitation and the influence of Glen Canyon Dam: Water Resources Research, v. 36, pp. 515-542.

Topping, D., Schmidt, J., Vierra, L., 2003, Computation and analysis of the instantaneous-discharge record for the Colorado River at Lee's Ferry, Arizona- May 8, 1921, through September 30, 2000: US Geological Survey Professional Paper 1677, 118 p.

Topping, D.J., Rubin, D.M., and Schmidt, J.C., 2005, Regulation of sand transport in the Colorado River by changes in the surface grain size of eddy sandbars over multi-year timescales: Sedimentology, v. 52, no. 5, p. 1133–1153, doi:10.1111/j.1365-3091.2005.00738.x.

Topping, D.J., Rubin, D.M., Grams, P.E., Griffiths, R.E., Sabol, T.A., Voichick, Nicholas, Tusso, R.B., Vanaman, K.M., and McDonald, R.R., 2010, Sediment transport during three controlled-flood experiments on the Colorado River downstream from Glen Canyon Dam, with implications for eddy-sandbar deposition in Grand Canyon National Park: U.S. Geological Survey Open-File Report 2010–1128, 111 p.

U.S. Department of the Interior, 1995, Operation of Glen Canyon Dam—Final Environmental Impact Statement, Colorado River Storage Project, Coconino County, Arizona: Salt Lake City, Utah, Bureau of Reclamation, Upper Colorado Regional Office, 337 p.

U.S. Department of the Interior, 1996, Record of Decision, Operation of Glen Canyon Dam—Final Environmental Impact Statement: Washington, D.C., Office of the Secretary of the Interior, Bureau of Reclamation, 15 p.

Walling, D. E., 2005, Tracing suspended sediment sources in catchments and river systems: Science of the Total Environment, v. 344, pp. 159-184.

Walling, D. E., 2013, The evolution of sediment source fingerprinting investigations in fluvial systems: Journal of Soils and Sediments, v. 13, pp. 1658-1675.

Walling, D.E., P.N. Owens, and G.J.L. Leeks, 1999, Fingerprinting Suspended Sediment Sources in the Catchment of the River Ouse, Yorkshire, UK. Hydrological Processes v. 13, pp. 955-975.

Walling, D.E., Woodward, JC., Nicholas, A.P., 1993, A multi-parameter approach to fingerprinting suspended sediment sources *in* Peters, N.E., Hoehn, E., Leibundgut, C., Tase, N., Walling, D. E., (eds) Tracers in hydrology: IAHS Publication, no. 215, pp. 329–338.

Webb, R.H.,Schmidt, J.C.,Marzolf, G.R.,Valdez, R.A., 1999, The controlled flood in Grand Canyon. Geophysical Monograph Series, v. 110, American Geophysical Union, Washington D.C.

Wiele, S.M., Andrews, E.D., and Griffin, E.R., 1999, The effect of sand concentration on depositional rate, magnitude, and location in the Colorado River below the Little Colorado River, *in* Webb, R.H., Schmidt, J.C., Marzolf, G.R., and Valdez, R.A., eds., The controlled flood in Grand Canyon: Washington, D.C., American Geophysical Union, Geophysical Monograph Series, v. 110, p. 131–145.

Williams, G.P., and Wolman, M.G., 1984, Downstream effects of dams on alluvial rivers: U.S. Geological Survey Professional Paper 1286, 83 p.

Wilson, C.G., R.A. Kuhnle, D.D. Bosch, J.L. Steiner, P.J. Starks, M.D. Tomer, and G.V. Wilson, 2008, Quantifying Relative Contributions from Sediment Sources in Conservation Effects Assessment Project Watersheds: Journal of Soil and Water Conservation, v. 63, no. 6, pp. 523-545.

Wright, S. A., Topping, D. J., Rubin, D. M., Melis, T. S., 2010, An approach for modeling sediment budgets in supply-limited rivers: Water Resources Research, v. 46, 18 p.

Yalcin, G.M., Narin, I., Soylak, M., 2008, Multivariate analysis of heavy metal contents of sediments from Gumusler creek, Nigde, Turkey: Environmental Geology, v. 54, pp. 1155–1163.

Year	Dates	Peak Discharge (cfs)	Duration at Peak Discharge
1996	Mar. 26 - Apr. 7	45,000	7 days
2004	Nov. 2 - 4	41,700	60 hours
2008	Mar. 6 - 8	42,800	60 hours
2012	Nov. 18 - 23	42,300	96 hours
2013	Nov. 11 - 16	34,100	96 hours
2014	Nov. 10 - 16	38,400	96 hours
2016	Nov. 7 - 12	36,800	96 hours

Table 1: Details of date, peak discharge, and duration at peak discharge for the 7 controlled flood events released from Glen Canyon Dam.

				2013 HFE		2014 HFE	
Lat.	Long.	RM	Site Name	Deposit Height (m)	Number of Samples	Deposit Height (m)	Number of Samples
36.8556	-111.6043	1.4	Paria Beach	0.20	3	-	-
36.8429	-111.6170	2.6	Cathedral	-	-	0.80	4
36.7716	-111.6563	8.1	Jackass	-	-	0.51	3
36.7715	-111.6563	8.9	9 Mile	1.00	7	1.30	5
36.6804	-111.7392	16.4	Hot Na Na	-	-	2.40	5
36.6128	-111.7600	22.1	22 Mile	1.30	5	0.70	4
36.5302	-111.8347	29.8	Silver Grotto	0.13	2	-	-
36.5159	-111.8476	30.4	30 Mile	1.30	5	1.90	7
36.4020	-111.8823	41.4	Buckfarm	2.80	4	1.15	4
36.3868	-111.8494	44.5	Eminence	1.65	6	2.20	3
36.3678	-111.8887	47.5	Saddle	-	-	0.90	1
36.3375	-111.8611	50.2	Dinosaur	2.25	7	-	-
36.2621	-111.8262	56.5	Kwagunt	-	-	0.90	4
36.2404	-111.8243	57.5	Malgosa	1.09	6	-	-

Table 2: Details of Marble Canyon sampling sites for 2013 and 2014 HFE deposits including location (latitude and longitude), river mile (RM), site name, deposit height in meters and number of samples taken from each deposit.

	Grain size fraction (µm)							
Population	**<63**	**63-90**	**90-125**	**125-180**	**180-250**	**250-355**	**355-500**	**>500**
Glen	11	14	14	14	14	14	13	5
Paria	2	45	45	45	45	42	31	13
Marble13	45	48	52	52	50	45	39	17
Marble14	0	37	37	37	37	33	28	4

Table 3: Total number of samples in each grain size fraction. Paria river suspended sediment samples obtained from the USGS were the >63 fraction, thus did not include any sediment <63 µm. The <63 µm fraction was excluded from all processing in anticipation of excluding that grain size in analyses. The >500 µm fraction had insufficient n in Glen Canyon to characterize the endmember, thus the fraction was excluded in the analyses.

	Mean reported concentration and standard error (ppm*)											
	63 - 90 µm											
Population	**Fe**	**Fe σ**	**Ca**	**Ca σ**	**Si**	**Si σ**	**P**	**P σ**	**S**	**S σ**	**K**	**K σ**
Glen Canyon	13254.5	974.3	15843.9	964.6	51071.8	1235.8	2611.8	132.2	491.8	18.4	906.8	17.5
Paria River	5747.1	68.2	18510.9	556.0	76073.0	2171.2	673.6	8.9	357.3	6.9	1661.4	65.0
Marble 2013	6462.4	168.3	15333.0	479.9	20875.6	1316.0	843.9	56.5	371.7	9.5	715.3	11.6
Marble 2014	6709.8	165.1	22856.7	740.3	65193.1	1789.6	1299.6	99.9	352.9	11.5	712.4	20.9
	90 - 125 µm											
Glen Canyon	9739.7	854.3	11597.8	664.3	57603.8	1515.6	1502.8	166.8	372.4	22.6	855.0	21.9
Paria River	4352.4	101.1	16100.4	454.2	60860.0	1380.2	605.9	7.8	354.6	6.6	1637.3	65.4
Marble 2013	4641.8	289.5	10847.8	419.6	18719.4	1165.6	502.3	13.5	369.4	11.0	682.6	9.8
Marble 2014	4169.0	95.8	15526.6	585.6	62553.3	1501.5	609.9	7.3	274.5	5.8	707.8	15.5
	125 - 180 µm											
Glen Canyon	4995.1	219.3	10478.5	772.2	57405.3	1442.3	615.1	11.9	258.9	6.4	826.5	15.6
Paria River	4458.0	139.2	19276.2	674.7	65008.8	1598.7	620.4	7.1	358.4	6.3	1579.0	62.8
Marble 2013	4320.3	144.5	10240.1	495.5	15666.0	718.0	484.1	4.6	365.2	9.5	700.7	9.7
Marble 2014	3796.5	112.1	15073.9	427.4	70466.0	2000.6	617.9	9.1	304.0	8.1	744.1	26.0
	180 - 250 µm											
Glen Canyon	4517.5	319.6	12033.0	855.3	58974.1	2087.1	647.5	13.9	262.2	7.8	853.4	20.7
Paria River	4035.1	205.1	14379.8	587.8	65484.5	1486.4	623.2	9.3	393.4	9.3	1649.5	63.5
Marble 2013	4199.8	113.7	9329.0	316.2	15957.3	781.9	444.7	5.6	383.0	11.1	662.7	10.4
Marble 2014	4413.2	214.4	15797.0	473.3	64010.9	1677.4	615.9	9.0	449.6	50.7	779.3	36.1
	250 - 355 µm											
Glen Canyon	4955.7	329.1	12210.4	825.1	58583.6	2014.7	639.1	12.1	299.3	15.5	823.5	16.6
Paria River	2969.9	168.6	12157.4	1177.3	66394.1	1509.6	638.5	13.7	428.3	18.4	1685.7	79.8
Marble 2013	4138.5	129.0	10650.1	330.8	17529.1	1059.5	464.9	6.3	389.6	12.2	644.0	11.5
Marble 2014	4135.7	139.1	14069.0	427.1	73598.7	2051.5	622.2	9.7	456.6	46.7	727.1	39.9
	355 - 500 µm											
Glen Canyon	6174.2	854.3	14966.9	1501.0	66564.7	3082.9	667.8	14.1	388.4	26.7	868.1	26.0
Paria River	2171.8	130.2	12310.9	1210.3	66346.9	1404.8	637.0	11.2	423.8	14.1	1658.6	96.0
Marble 2013	3581.3	115.0	11327.1	321.8	22933.1	1558.8	461.4	7.7	412.7	17.2	614.8	10.4
Marble 2014	4935.3	262.6	16969.2	631.5	69477.5	1867.9	615.9	11.8	500.4	42.0	762.9	27.1

Table 4: Mean and standard error of all elements from which sample-specific ratios were calculated, averaged, and utilized in the fingerprints. Marble Canyon sand divided into samples specific to the 2013 and 2014 deposits.

	Mean reported concentration and standard error (ppm*)									
	63 - 90 µm									
Population	**Cl**	**Cl σ**	**Ti**	**Ti σ**	**Rb**	**Rb σ**	**Sr**	**Sr σ**	**Zr**	**Zr σ**
Glen Canyon	11290.7	134.5	1940.0	127.3	42.1	0.3	99.3	1.0	2971.6	474.5
Paria River	13604.1	139.8	920.7	11.7	47.0	0.3	77.3	0.5	134.3	6.7
Marble 2013	9249.6	84.5	1039.6	27.9	42.2	0.2	77.5	0.8	543.8	50.4
Marble 2014	11638.5	134.2	1160.4	29.6	42.4	0.3	79.9	0.8	538.1	52.6
	90 - 125 µm									
Glen Canyon	8807.2	223.2	1290.4	107.9	33.9	0.7	79.9	1.3	694.5	109.8
Paria River	11293.2	152.5	685.7	15.0	40.6	0.4	59.7	0.7	57.7	2.0
Marble 2013	7897.2	95.8	680.7	30.1	37.3	0.4	54.8	0.9	124.9	19.1
Marble 2014	10289.0	151.5	660.4	14.8	38.6	0.5	58.3	1.0	109.9	6.0
	125 - 180 µm									
Glen Canyon	7226.5	247.9	726.3	32.7	28.9	0.8	71.8	1.9	83.8	7.2
Paria River	9848.4	169.6	631.3	19.8	35.8	0.5	58.1	0.9	41.3	1.0
Marble 2013	6563.1	117.2	605.6	21.4	31.5	0.6	49.8	1.1	55.2	2.0
Marble 2014	9226.1	169.3	563.9	17.7	33.6	0.6	51.5	0.9	52.3	1.8
	180 - 250 µm									
Glen Canyon	7103.6	299.9	578.6	40.3	29.5	1.0	73.9	2.5	54.3	2.9
Paria River	7791.4	195.2	564.8	29.4	28.5	0.7	48.5	1.2	35.6	0.6
Marble 2013	5201.7	100.6	591.4	20.9	24.1	0.4	41.5	0.6	51.7	3.0
Marble 2014	7921.0	177.5	646.2	36.1	29.0	0.7	51.0	1.2	57.7	4.2
	250 - 355 µm									
Glen Canyon	7658.6	312.1	608.4	44.9	32.1	1.1	80.1	2.5	63.5	5.0
Paria River	5240.9	175.3	436.7	23.8	17.7	0.5	36.3	1.4	31.7	0.6
Marble 2013	4386.8	120.1	502.8	15.1	20.5	0.5	41.8	0.9	45.3	1.5
Marble 2014	6446.1	172.2	581.2	22.9	22.9	0.6	45.1	1.0	51.6	2.7
	355 - 500 µm									
Glen Canyon	9118.0	405.3	718.0	81.7	39.7	1.9	88.9	4.8	72.2	11.2
Paria River	3456.8	171.1	308.2	14.2	11.0	0.5	29.6	1.2	28.0	0.7
Marble 2013	3647.9	115.0	418.8	11.5	18.0	0.5	42.4	1.1	39.2	0.8
Marble 2014	6203.2	244.1	576.4	31.1	22.1	1.1	51.7	2.2	50.9	2.5

*based on values reported directly by the XRF, not absolute. See text for details

Grain Size	*n* ratios	Eligible Ratios
63 - 90	35	Fe/Ca, Fe/S, Fe/Cl, Fe/K, Fe/Rb, Fe/Sr, Fe/Zr, Ca/Ti, Ca/Zr, Si/P, Si/S, Si/Ti, Si/Zr, P/S, P/Cl, P/K, P/Ti, P/Rb, P/Sr, P/Zr, S/Cl, S/K, S/Ti, S/Zr, Cl/Ti, Cl/Zr, K/Ti, K/Sr, K/Zr, Ti/Rb, Ti/Sr, Ti/Zr, Rb/Sr, Rb/Zr, Sr/Zr
90 - 125	34	Fe/Ca, Fe/S, Fe/Cl, Fe/K, Fe/Ti, Fe/Rb, Fe/Sr, Fe/Zr, Ca/Ti, Ca/Sr, Ca/Zr, Si/P, Si/Cl, Si/Ti, Si/Zr, P/S, P/Cl, P/K, P/Zr, S/Ti, S/Sr, S/Zr, Cl/Ti, Cl/Sr, Cl/Zr, K/Ti, K/Sr, K/Zr, Ti/Rb, Ti/Sr, Ti/Zr, Rb/Sr, Rb/Zr, Sr/Zr
125 - 180	30	Fe/Ca, Fe/S, Fe/K, Fe/Rb, Fe/Zr, Ca/P, Ca/S, Ca/K, Ca/Ti, Ca/Rb, Ca/Sr, Ca/Zr, Si/Cl, P/K, P/Ti, P/Sr, P/Zr, S/Ti, S/Sr, S/Zr, Cl/Ti, Cl/Sr, Cl/Zr, K/Ti, K/Sr, K/Zr, Ti/Rb, Ti/Zr, Rb/Zr, Sr/Zr
180 - 250	18	Fe/S, Fe/Zr, Ca/Rb, Ca/Sr, Ca/Zr, Si/Cl, P/Cl, P/Sr, S/Ti, S/Sr, S/Zr, Cl/Sr, K/Rb, K/Sr, K/Zr, Ti/Zr, Rb/Sr, Rb/Zr
250 - 355	25	Fe/Ca, Fe/S, Fe/Ti, Ca/Ti, Ca/Rb, Ca/Sr, Ca/Zr, Si/Cl, Si/Rb, Si/Sr, P/K, P/Rb, P/Sr, S/K, S/Ti, S/Rb, S/Sr, S/Zr, Cl/K, Cl/Rb, Cl/Sr, K/Rb, K/Sr, Ti/Zr, Rb/Sr
355 - 500	31	Fe/Ca, Fe/S, Fe/Cl, Ca/K, Ca/Ti, Ca/Rb, Ca/Sr, Ca/Zr, Si/Cl, Si/K, Si/Rb, Si/Sr, P/K, "P/Rb, P/Sr, /Zr, S/K, S/Ti, S/Rb, S/Sr, S/Zr, Cl/K, Cl/Rb, Cl/Sr, Cl/Zr, K/Rb, Ti/Rb, Ti/Sr, Rb/Sr, Rb/Zr, Sr/Zr

Table 5: Number and list of ratios eligible for use in each grain size-specific fingerprint.

Grain Size (μm)	PC1	PC2	PC3	PC4	PC5	Variance explained by PC1 and PC2
63-90	0.630	0.133	0.074	0.051	0.033	0.764
90-125	0.572	0.135	0.082	0.062	0.048	0.707
125-180	0.404	0.191	0.167	0.092	0.053	0.595
180-250	0.426	0.210	0.140	0.097	0.043	0.636
250-355	0.440	0.192	0.114	0.074	0.047	0.632
355-500	0.465	0.184	0.119	0.058	0.040	0.649

Table 6: Proportion of the total original variance explained by each principal component (PC) in each grainsize and cumulative original variance explained by PC1 and PC2.

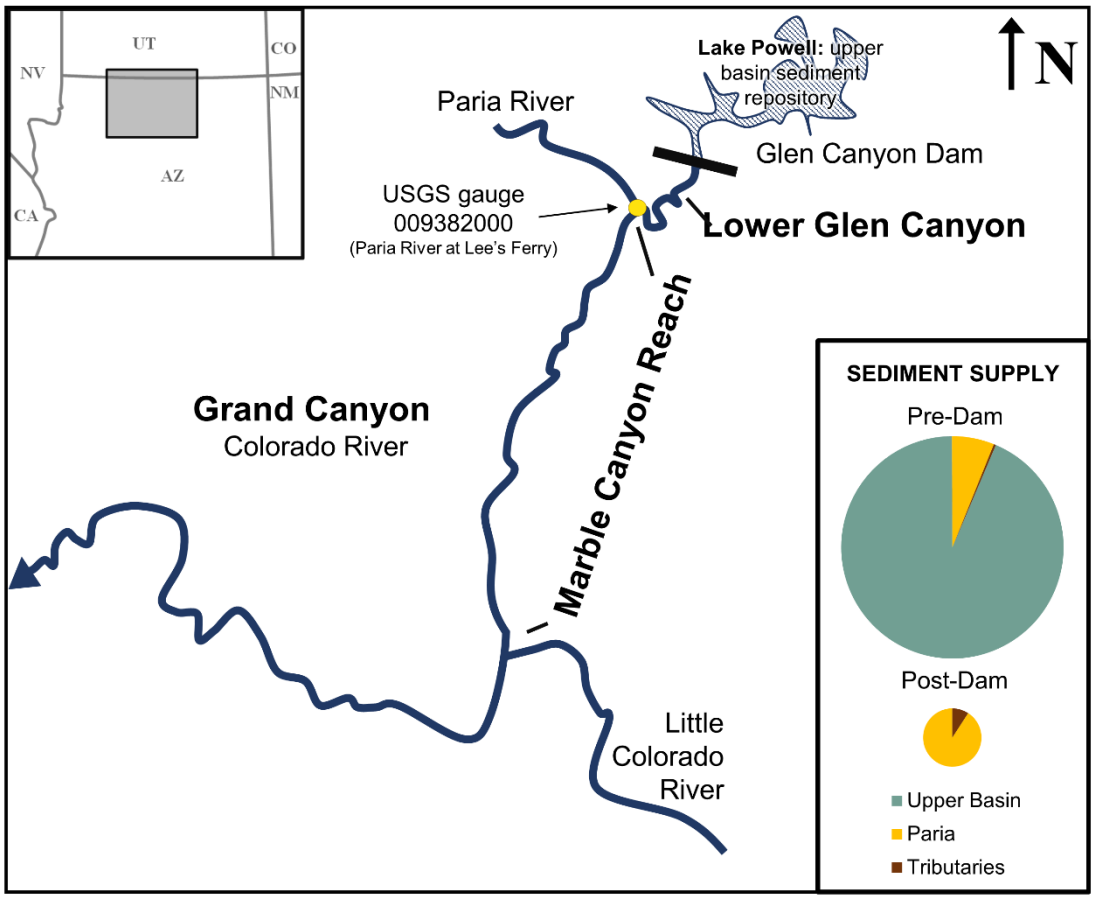

Figure 1: Geometry of Colorado River system below Glen Canyon Dam. Lower Glen Canyon is the 15-mile reach downstream of Glen Canyon Dam; the Marble Canyon reach of Grand Canyon starts at Lee's Ferry (yellow circle) and ends at the Little Colorado River confluence. USGS gauge Paria River at Lee's Ferry (09382000) location indicated by yellow circle.

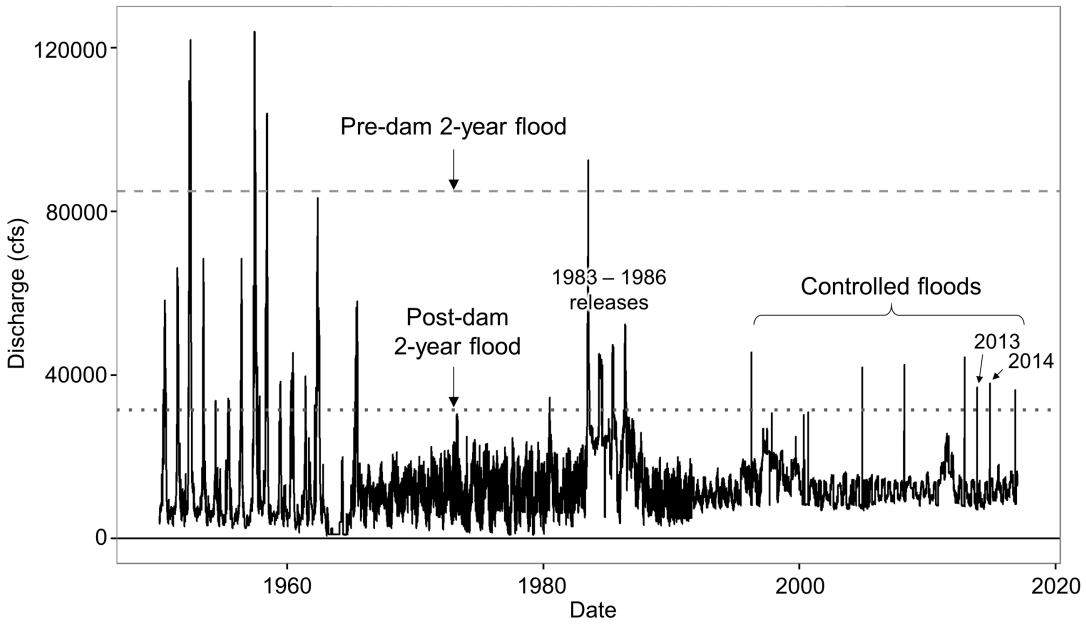

Figure 2: Colorado River at Lee's Ferry discharge from 1950-present, recorded at USGS gauge 09380000. Data source: https://www.gcmrc.gov/discharge_qw_sediment/.

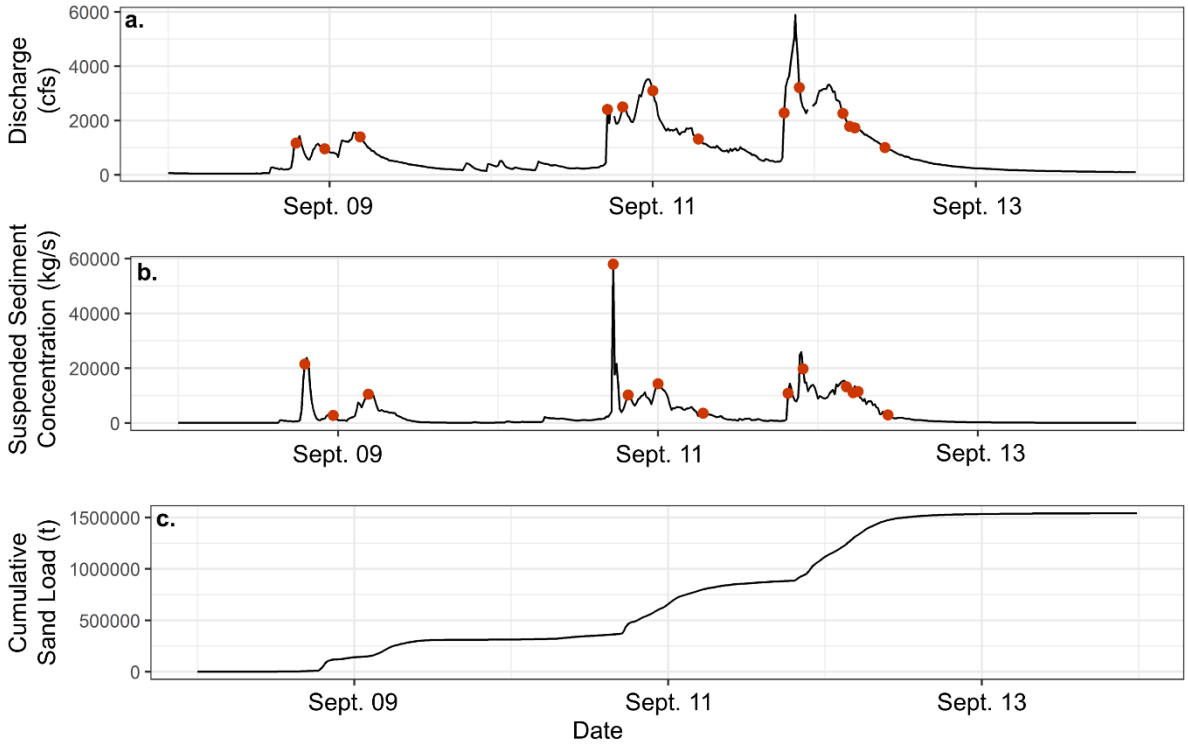

Figure 3: (a) Paria River discharge (cfs), (b) suspended sediment concentration (kg/s), and cumulative sand load (t) delivered to the main stem Colorado River for the period of September 8-13, 2013. Red dots indicate suspended sediment samples used in this study. The cumulative sediment load increases drastically with each flash flood, with comparatively little transport during interim flows. Note that discharge and suspended concentration can act independently of each other. Data source: www.gcmrc.gov/discharge_qw_sediment/.

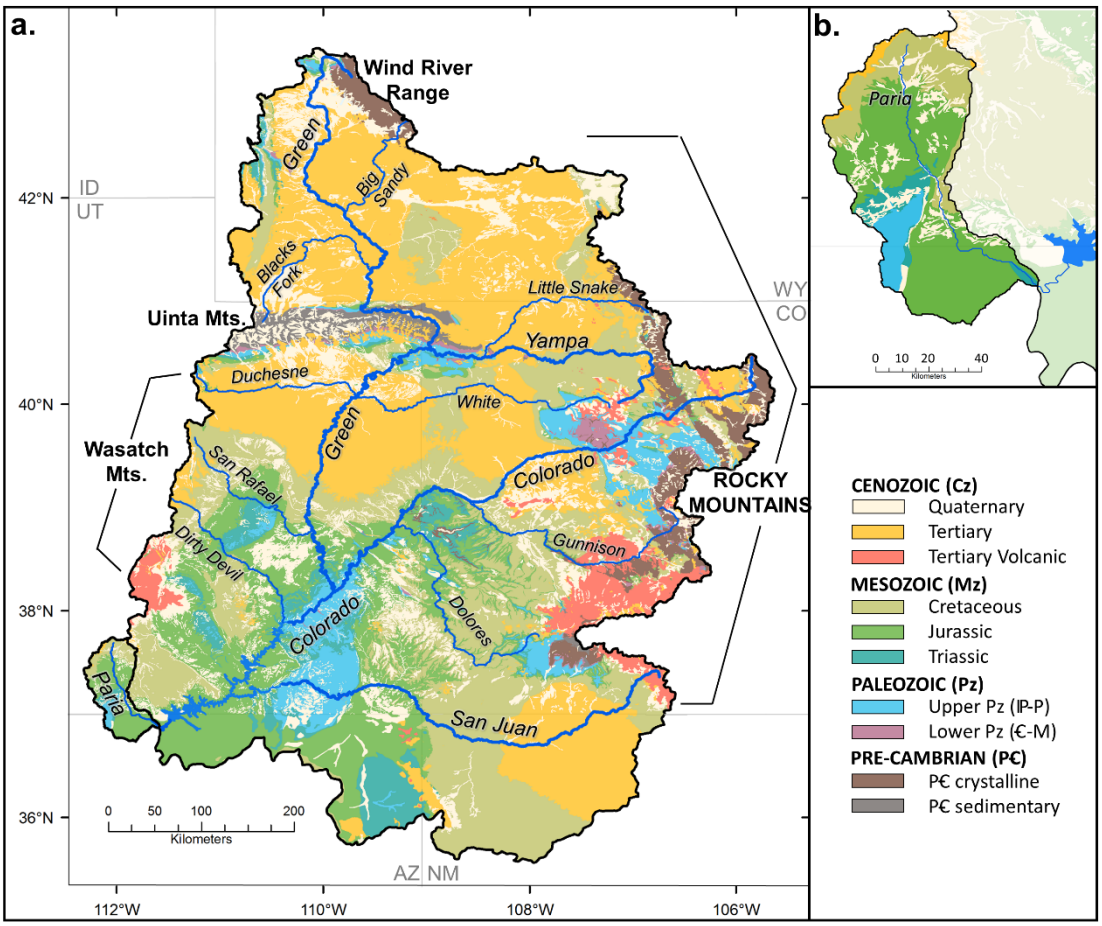

Figure 4: Geology of Upper Colorado (a) and Paria River (b) watersheds. The Colorado and its tributaries (the Yampa, San Juan Rivers, and their associated tributaries, the Little Snake, White, Gunnison, and Dolores Rivers) drain the pre-Cambrian crystalline basement, Paleozoic and Mesozoic sedimentary strata, and Tertiary volcanic rocks. The Paria River drainage is restricted to Paleozoic and Mesozoic strata. Data source: Lehner et al., 2006; Stoeser et al., 2007, Ludington et al., 2007.

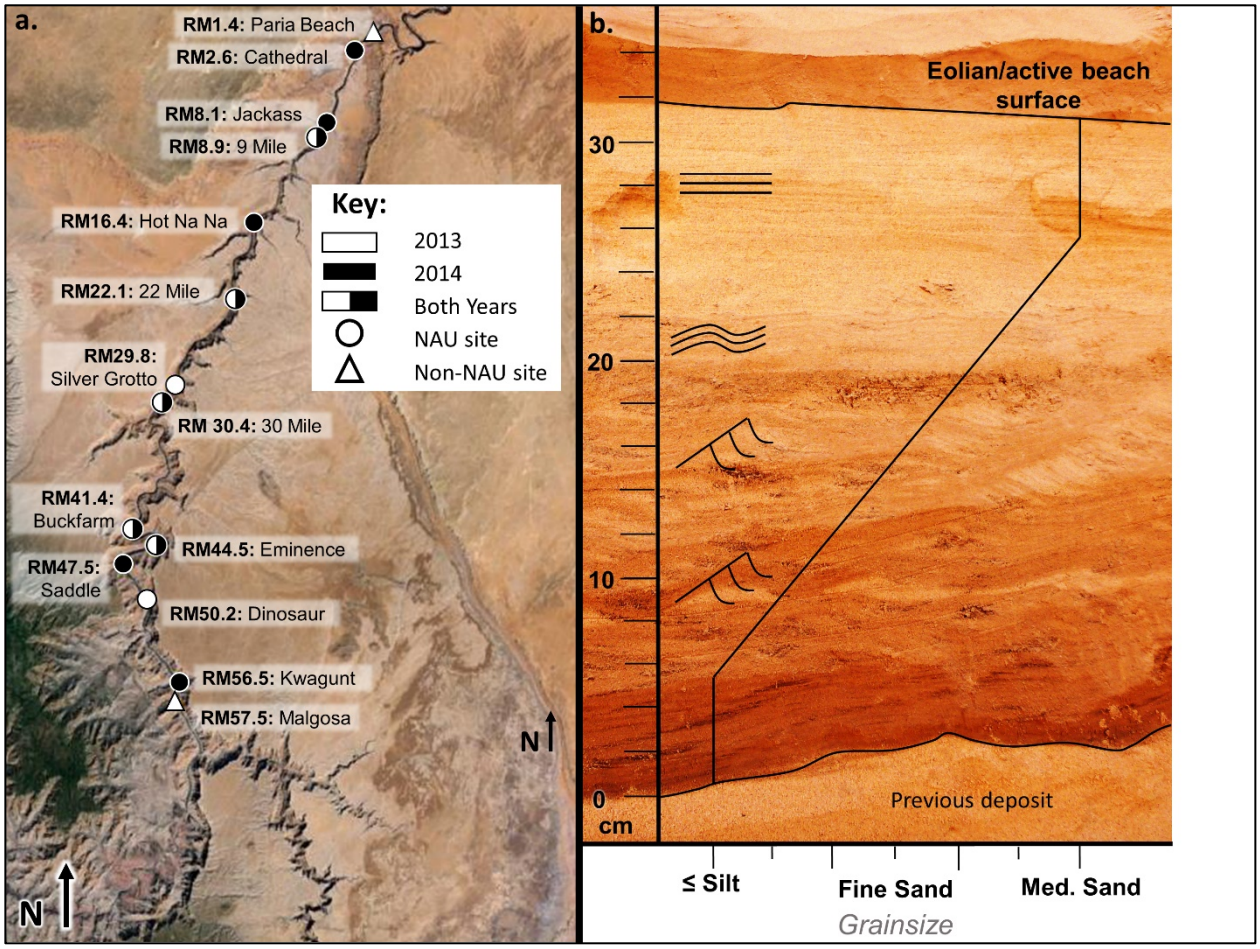

Figure 5: (a) Sample locations for Marble Canyon HFE deposits. Color indicates year, shape indicates if the deposit is one of the long-term study sites for the Northern Arizona University Sandbar Studies program. Base photo source: Landsat, accessed via GoogleEarth. (b) Idealized stratigraphic column for Marble Canyon deposits: the transition from climbing ripples up upper planar beds indicates a Froude transition from sub- to supercritical flow, likely due to decreased depth following deposition.

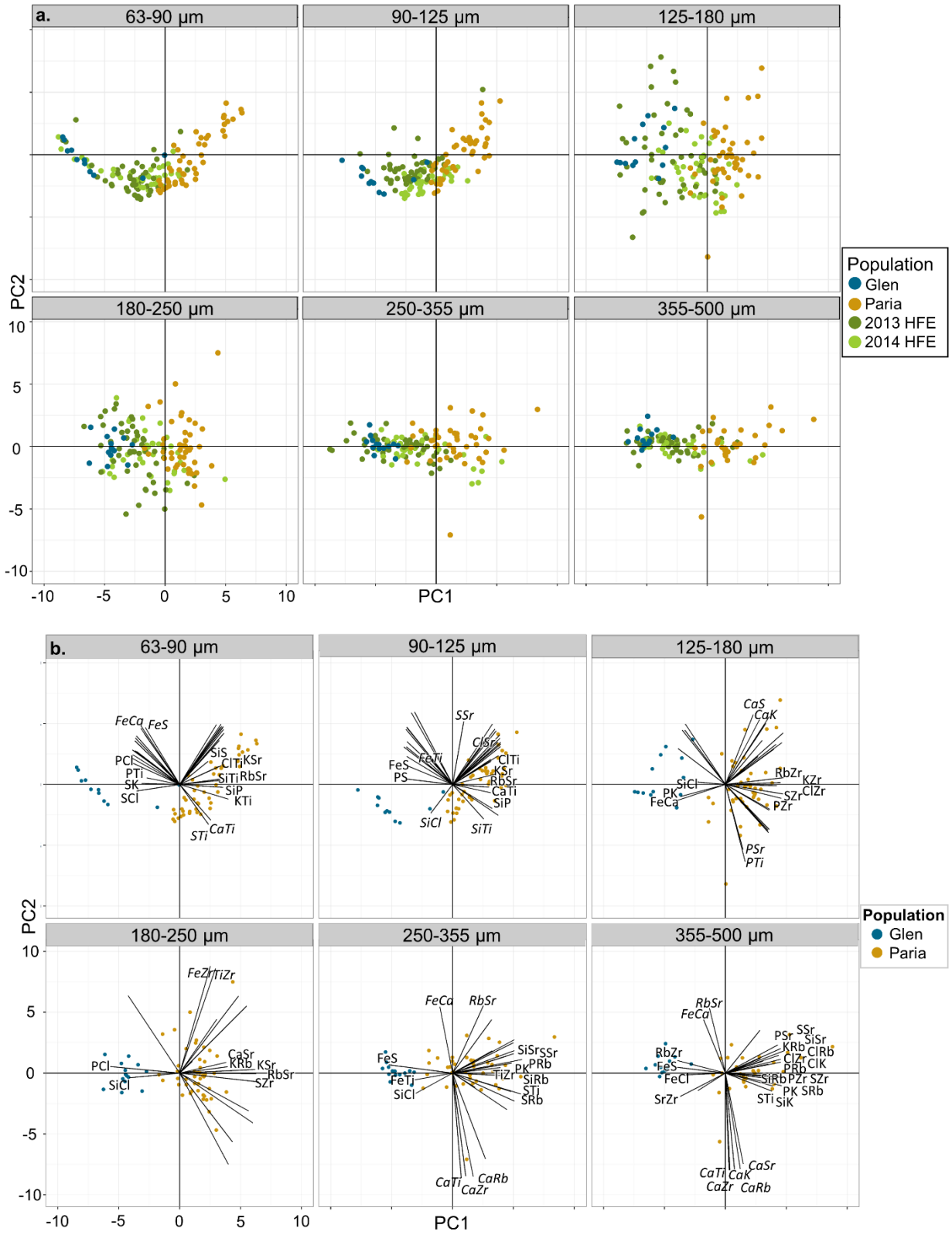
a.
63-90 µm
90-125 µm
125-180 µm
180-250 µm
250-355 µm
355-500 µm
PC2
PC1
Population
Glen
Paria
2013 HFE
2014 HFE
b.
63-90 µm
90-125 µm
125-180 µm
180-250 µm
250-355 µm
355-500 µm
PC2
PC1
Population
Glen
Paria

Figure 6: (a) Endmember and mixed population values for PC1 and PC2, individual boxes are labeled by the grain size fraction (in µm) they represent. (b) PC1 and PC2 values for endmember populations and loadings (black lines) indicating the ratios which most heavily influence each PC; straight text indicates ratios for PC1, italics for PC2.

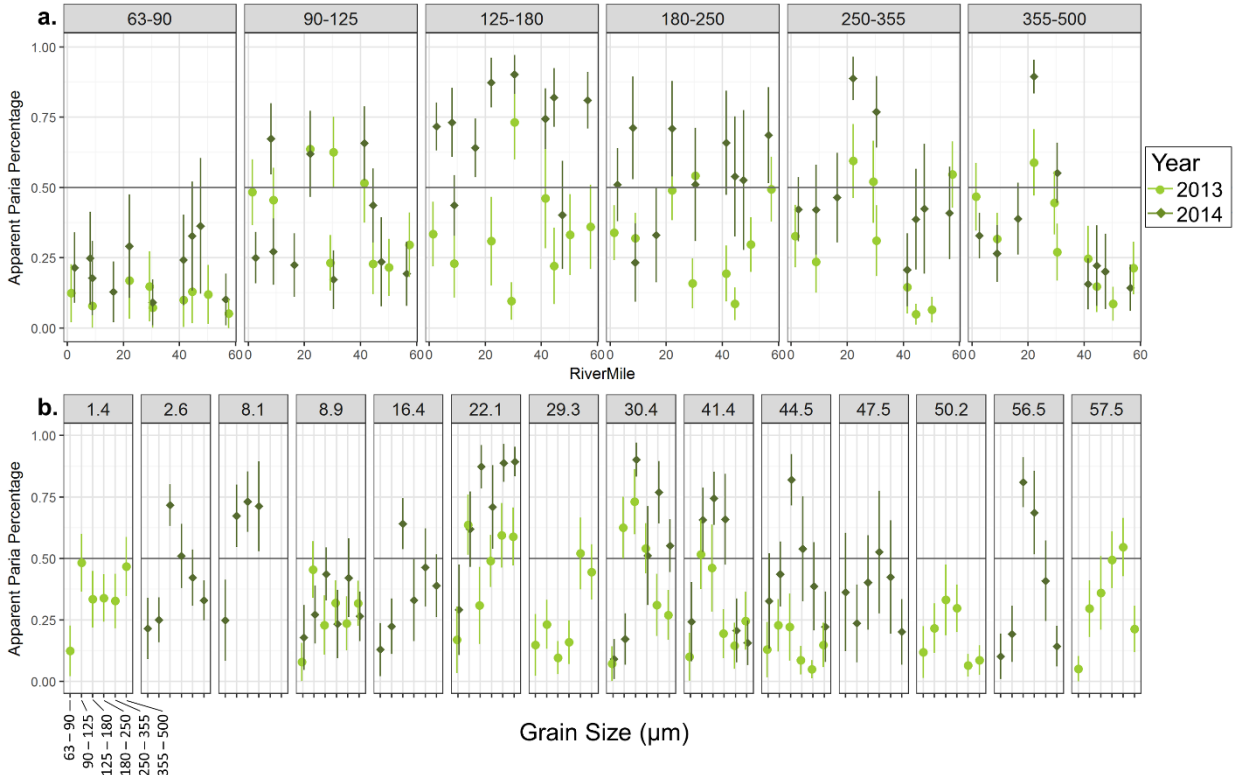

Figure 7: Mixing model results for each sample, sorted by grain size (a) and river mile (b). Error bars indicate the standard error of that mean across all estimates of APP for a specific grain size within one deposit.

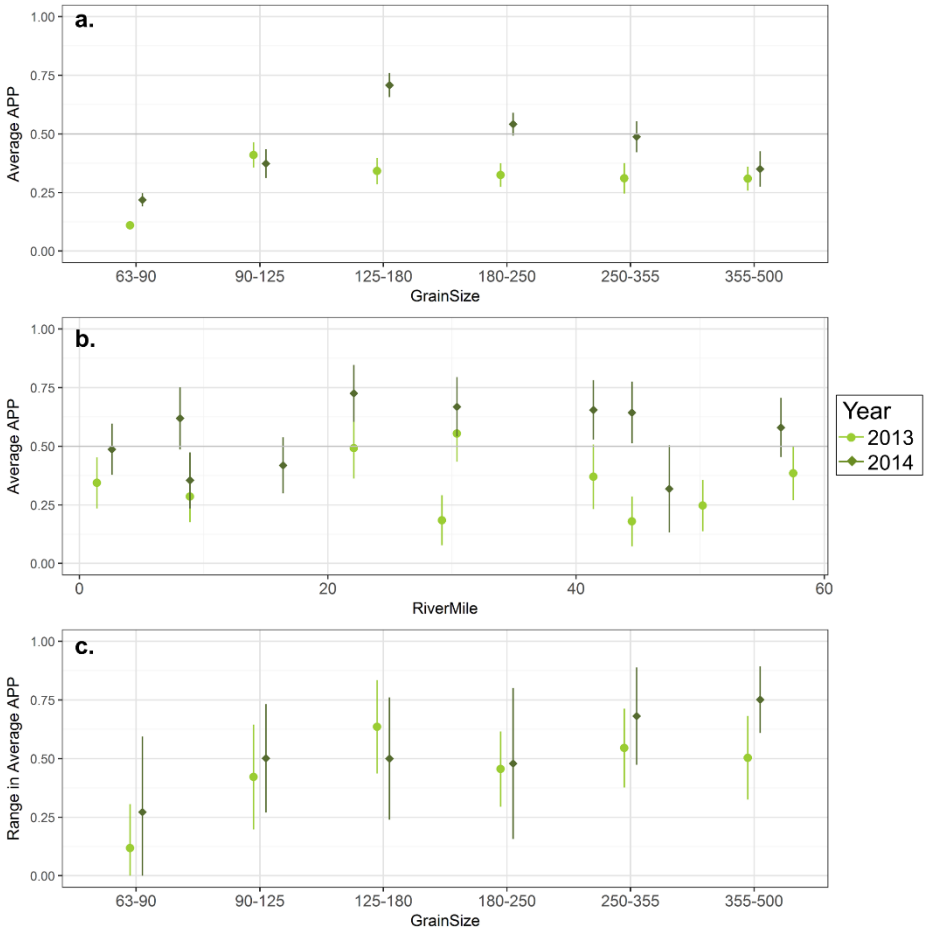

Figure 8: Average APP for each grain size (a), deposit (b), and range in average APP for each grain size fraction in both years (c); color and shape indicate year. Error bars in (a) and (b) represent the standard errors of each APP estimate for one grain size of one deposit (those shown in Fig. 7), propagated through an arithmetic average of all estimates per year by grain size and river mile, respectively. Error bars in (c) indicate the compound uncertainty of the difference between the maximum and minimum APP values for each year shown in Fig. 7a.

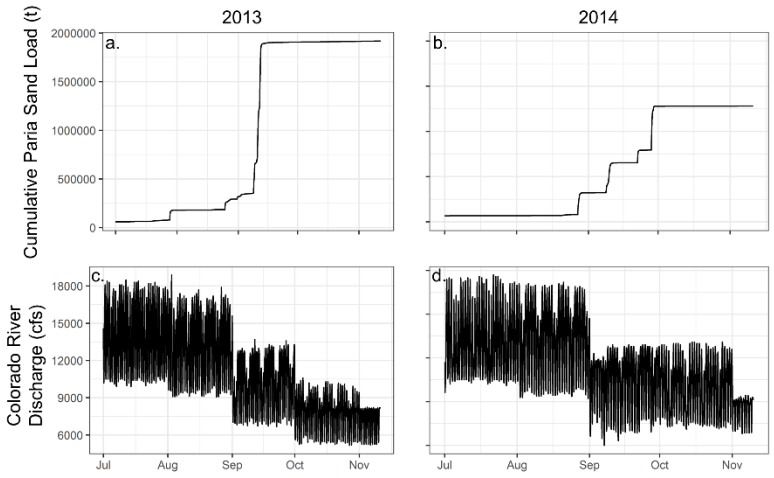

Figure 9: Cumulative sand load delivered by the Paria River to the mainstem Colorado July 1st to the controlled floods in November of 2013 (a) and 2014 (b), and corresponding Colorado River discharge measured at USGS gauge 0009380000 (Colorado River at Lee's Ferry) in the same time spans of 2013 (c) and 2014 (d).

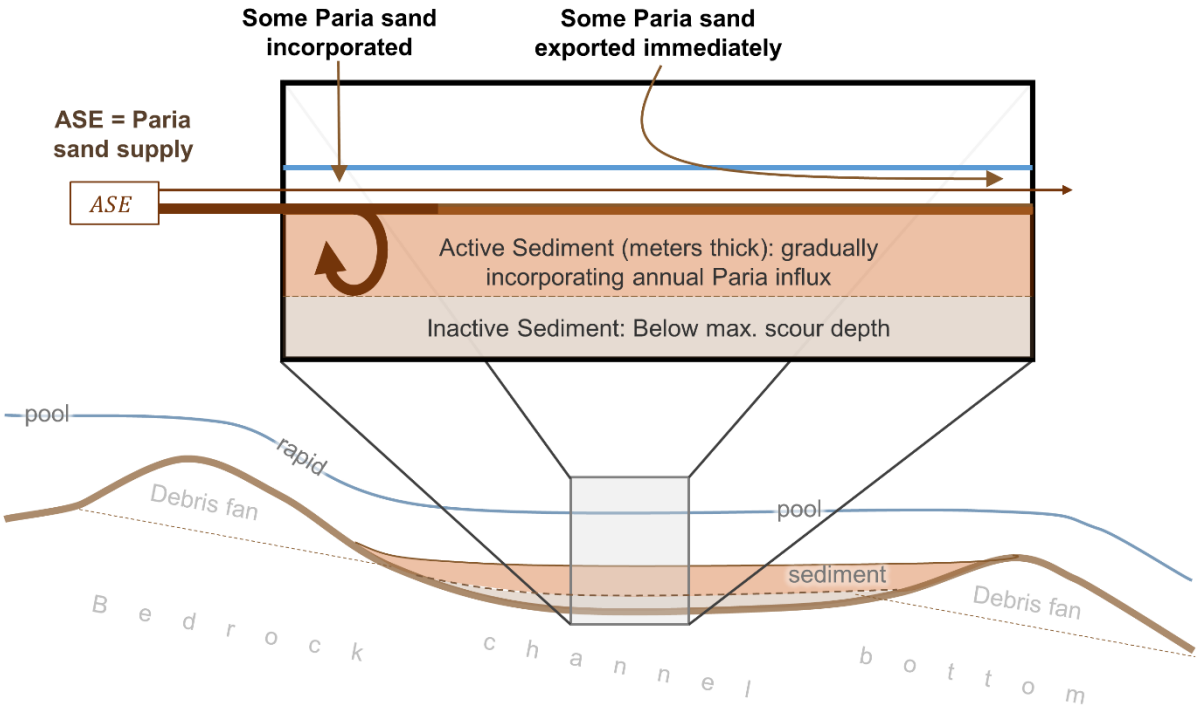

Figure 10: Mass balance for retention of Paria-derived sand in Marble Canyon active storage. ASE is the Paria sand enrichment available for transport immediately prior to HFEs. See Equation 1 and following discussion for details.

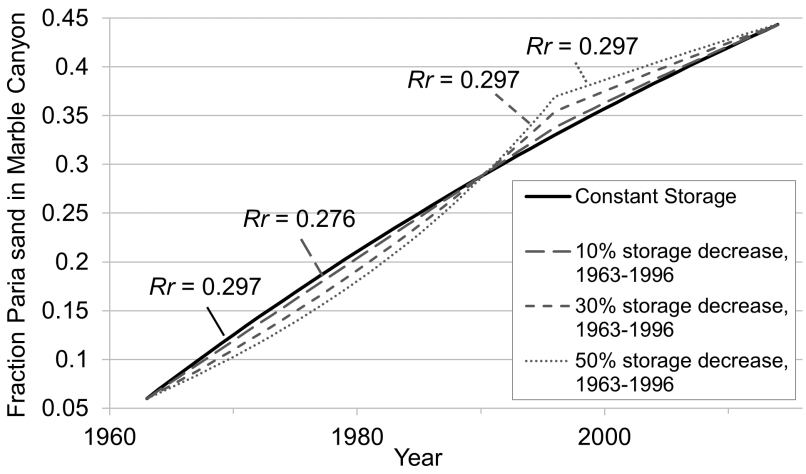

Figure 11: Graphs of increasing Paria sand fraction within Marble Canyon active storage. A scenario assuming constant storage is compared to (a) scenarios with a 10%, 30%, and 50% decrease in storage over the years 1963-1996, before holding constant when management began in 1996. Annotations indicate the Paria sand retention rate (*Rr*) required to reach the 44% Paria sand by 2014 under these different storage scenarios.